Introduction

The heterogeneous nature of breast cancer has been demonstrated by gene expression profiling using the DNA microarray technique [1–3]. Genetically, invasive breast cancers have been classified into distinct intrinsic subtypes comprising luminal A, luminal B, ERBB2 (HER2), basal-like, and normal breast subtypes [1–3], which demonstrate characteristic immunohistochemical features and clinical behavior [4–8]. Both basal-like and normal breast subtypes are immunohistochemically characterized by lack of expression of the estrogen receptor (ER), progesterone receptor (PgR), and HER2, and thus are also categorized as triple-negative breast cancer (TNBC). TNBC, which accounts for 10–15% of all breast cancers, tends to show visceral metastasis and aggressive clinical behavior [9].

TNBC is unresponsive to specific targeted therapies such as trastuzumab for HER2-positive breast cancer, or hormonal therapy for hormone-receptor-positive breast cancer. In cases of operable TNBC, only systemic chemotherapy has been shown to be effective in an adjuvant or neoadjuvant setting. Although patients with TNBC are more likely to achieve a pathological complete response (pCR) after neoadjuvant chemotherapy (NAC) than patients with the luminal subtypes, and pCR is correlated with an excellent clinical outcome, TNBC patients with residual disease after NAC have a poor prognosis [10, 11]. However, the factor that determines sensitivity to chemotherapy in patients with TNBC is uncertain.

TNBC itself may show heterogeneous characteristics including basal-like and normal breast subtypes, as judged from gene expression profiles [1–3]. Accordingly, it is important to investigate the pathological factors associated with response to chemotherapy in patients with TNBC.

The aim of the present study was to identify the factors that predict pCR after NAC in patients with TNBC by examination of histological parameters including histological grade and type, the presence of tumor-infiltrating lymphocytes (TIL), and tumor cell apoptosis, as well as immunohistochemical parameters including basal-like markers and p53.

Materials and methods

Patients and tissue samples

Among 474 patients who received NAC and subsequent surgical therapy for stage II–III invasive breast carcinoma between 1999 and 2007, 102 (22%) had TNBC. Originally, we planned to compare 100 TNBCs with 100 non-TNBCs as controls on the basis of matching for age (±5years) and clinical stage (II and III). In the 100 control cases, we planned to include 50 cases of the HR−/HER2+ subtype (HER2 positive and ER/PgR negative in routine immunohistochemistry) and 50 cases of the HR+/HER2− subtype (ER and/or PgR positive but HER2 negative in routine immunohistochemistry). From these patients, sufficient CNB specimens before NAC were available from 92 tumors of TNBC, 42 tumors of the HR−/HER2+ subtype, and 46 tumors of the HR+/HER2− subtype. Clinical characteristics of all patients were obtained from the medical records. All patients received neoadjuvant anthracycline-based regimens (adriamycin 60 mg/m^2 plus cyclophosphamide 600 mg/m^2 (AC) or cyclophosphamide 600 mg/m^2 plus epirubicin 100 mg/m^2/5-fluorouracil 600 mg/m^2 (CEF)) alone, taxane-based regimens (weekly paclitaxel 80 mg/m^2, or triweekly docetaxel 75 mg/m^2) alone, or anthracycline and taxane sequentially or concurrently (adriamycin 50 mg/m^2 plus docetaxel 60 mg/m^2 (AT), AC or CEF followed by weekly paclitaxel or triweekly docetaxel). Trastuzumab was not used for the 42 patients with tumors of HR−/HER2+ subtype, because the use of trastuzumab for neoadjuvant therapy of primary breast cancer was not approved in Japan. The patients have been followed up for 64.8 months on an average (7.2–138.2 months). All specimens were formalin-fixed and paraffin-embedded, and 4-μm-thick sections were prepared for hematoxylin and eosin staining and immunohistochemistry (IHC) and were reviewed by two observers including an experienced pathologist (T.H.). The present study was approved by the Institutional Review Board of the National Cancer Center.

Histopathological evaluation

Pathological therapeutic effect was assessed for resected primary tumors after NAC. Pathological complete response (pCR) was defined as the absence of all invasive disease in the breast tumor according to the National Surgical Adjuvant Breast and Bowel Project (NSABP) B-18 protocol [12]. In addition, we defined quasi-pCR (QpCR) as the absence of invasive tumor or only focal residual invasive carcinoma cells in the primary site [13]. In Japan, Breast Cancer Research Group (JBCRG) 01 study, QpCR after NAC was shown to be correlated with better patient prognosis in comparison with non-QpCR [13]. Furthermore, we took into consideration both the pCR in the primary tumor and no residual tumor in axillary lymph nodes as another classification for histopathological therapeutic effect [14, 15].

Histopathological assessment of predictive factors was made for CNB specimens. Histopathological parameters examined included histological grade [16], histological type [17], presence of tumor-infiltrating lymphocytes (TIL), apoptosis, and correlation of these parameters with intrinsic subtypes and pCR. Histological grade was assigned on the basis of the criteria of Elston and Ellis.

For the evaluation of TIL, both areas of stroma infiltrated by lymphocytes (proportional score) and intensity of lymphatic infiltration (intensity score) were taken into consideration. Proportional scores were defined as 3, 2, 1, and 0 if the area of stroma with lymphoplasmacytic infiltration around invasive tumor cell nests were >50, >10–50, ≤10%, and absent, respectively. Intensity scores were defined as 2, 1, and 0, if the intensity of lymphatic infiltration was marked, mild, and absent, respectively (Fig. 1). Lymphocyte infiltration surrounding non-invasive tumor cells was not taken into account. The proportional and intensity scores were summed for each tumor, and the TIL score was classified as high if the sum was 3–5, whereas the TIL score was classified as low if the sum was 0–2. As criteria for apoptosis, scores were defined as 2, 1, and 0 if apoptotic cells (arrows in Fig. 2) were>10 per 10 high-power fields (HPFs) using 40× objective lens, 5–9 per 10 HPFs, and less than 5 per 10 HPFs, respectively.

Immunohistochemistry (IHC)

IHC was performed for CNB specimens using the following primary antibodies: anti-ER (clone 1D5; Dako), anti-PgR (clone PgR636; Dako), anti-HER2 (polyclonal, HercepTest II, Dako), anti-p53 (clone DO-7; Dako), anti-cytokeratin (CK) 5/6 (clone D5/16 B4; Dako), anti-CK14 (NCL-LL002, Novocastra), and anti-EGFR (pharmDX, clone 2-18C9, Dako).

Because ER, PgR, and HER2 tests had been performed by various antibodies and methods, these tests were re-tested again according to standardized antibodies and methods in the present study. The sections were deparaffinized, subjected to antigen retrieval by incubating in target retrieval solution, high pH (Dako) for 40 min at 95°C for ER and PgR, in sodium citrate buffer (pH 6.0) with a microwave oven for 15 min at 97°C for CK14, in sodium citrate buffer (pH 6.0) with a water bath for 15 min at 98°C for CK5/6, or by autoclaving in sodium citrate buffer (pH 6.0) for 20 min at 121°C for p53, then allowed to cool at room temperature. Endogenous peroxidase and non-specific staining were blocked in 2% normal swine serum (Dako). The slides were incubated with primary antibodies at 4°C overnight and then reacted with a dextran polymer reagent combined with secondary antibodies and peroxidase (Envision Plus, Dako) for 2 h at room temperature. Specific antigen–antibody reactions were visualized using 0.2% diaminobenzidine tetrahydrochloride and hydrogen peroxide. Counterstaining was performed using Mayer's hematoxylin. For the HER2 and EGFR kits, immunohistochemistry was performed in accordance with the protocol recommended by the manufacturer.

ER and PgR were judged as positive if the Allred score was ≥3 and as negative if the Allred score was ≤2 [18]. HER2 protein overexpression was judged as positive when the score was 3+, equivocal when the score was 2+, and negative when the score was 0 or 1+ in accordance with the ASCO/CAP recommendation [19]. TNBC was defined as negative for ER, PgR, and HER2, while the HR+/HER2− subtype was defined as positive for ER or PgR and negative for HER2, and the HR−/HER2+ subtype was defined as negative for ER and PgR, and positive for HER2. The basal-like subtype was defined as CK5/

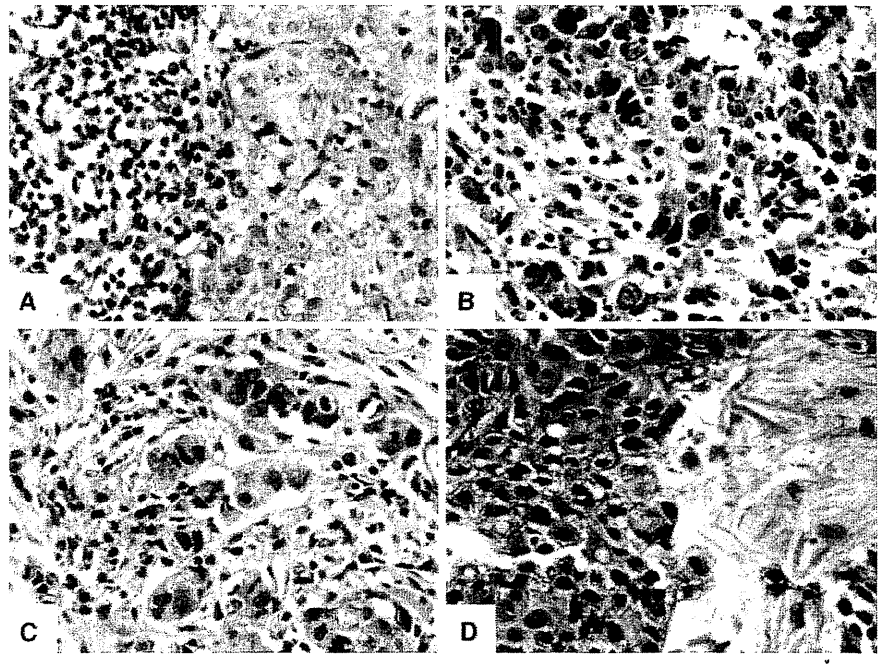

Fig. 1 Histophathological features of tumor-infiltrating lymphocytes (TILs). **a** High TIL score (proportional score 3+ intensity score 2); **b** High TIL score (proportional score 2+ intensity score 2); **c** Low TIL score (proportional score 1+ intensity score 2); **d** Low TIL score (proportional score 0, intensity score 0). Original magnification: 400×

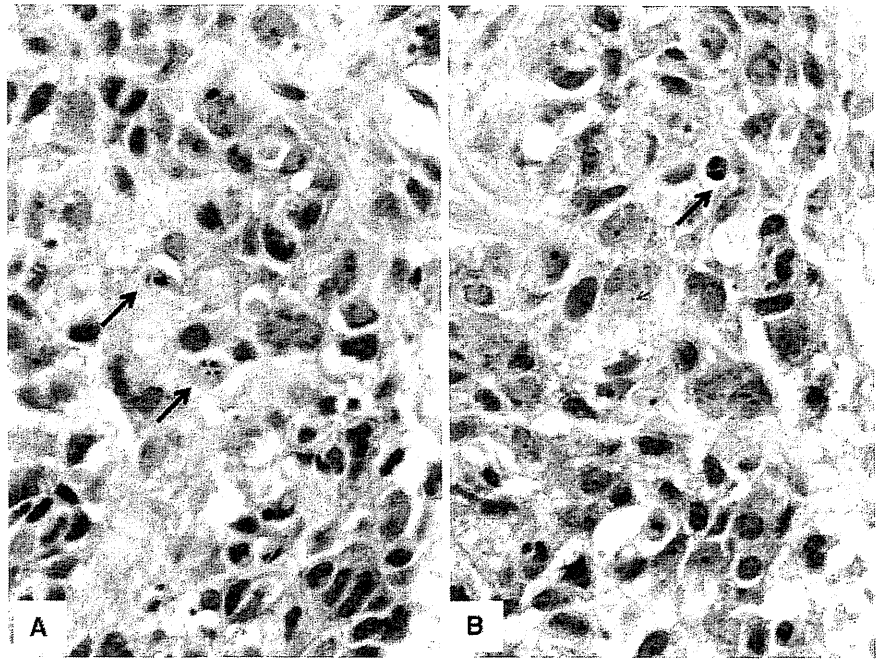

Fig. 2 Histophathological features of breast carcinoma with apoptosis (**a**, **b**) (*arrows*: apoptosis) Original magnification: 400×

6 > 1%, CK14 > 1%, or EGFR > 1%. For reference, data based on the criteria CK5/6 > 10%, CK14 > 10%, or EGFR > 10% were also acquired. p53 was scored using the Allred score and was regarded as positive when ≥5.

Statistical analyses

Statistical analyses were performed using SPSS software. Patients' characteristics were compared between subgroups using the chi-squared test or Fisher's exact test for categorical variables, and Kruskal–Wallis test for continuous variables. Association of pathological parameters, including a basal-like subtype, with pCR, QpCR, or pCR and no residual axillary tumor were evaluated using the chi-squared test or Fisher's exact test. Predictive ratio of pCR, QpCR, or pCR plus residual axillary metastasis by clinicopathological parameters were analyzed using the univariate and multivariate logistic regression models. Survival curves of patients were drawn using Kaplan–Meier method, and statistical difference between survival curves were calculated by using the log-rank test. In all analyses, differences were considered significant at $P < 0.05$.

Results

We confirmed immunohistochemically that all 92 tumors were TNBC, 42 of 50 were of the HR−/HER2+ subtype, and 46 of 50 were of the HR+/HER2− subtype. A total of 180 specimens were investigated in this study. The characteristics of the patients are presented in Tables 1 and 2.

Clinicopathological characteristics and subtypes

In tumors with the TNBC and HR−/HER2+ subtype, the frequencies of the basal-like subtype were 59% (54 of 92) and 43% (18 of 42), respectively, compared with only 7% (3 of 46) in the HR+/HER2− subtype. Therefore, the incidence of the basal-like subtype was significantly higher in TNBC or in the HR−/HER2+ subtype than in the HR+/HER2− subtype ($P < 0.001$). Similarly, the frequency of p53 expression was significantly higher in TNBC (63%, 58 of 92) and the HR−/HER2+ subtype (62%, 26 of 42) than in the HR+/HER2− subtype (26%, 12 of 46) ($P < 0.001$). Tumors of histological grade 3 were more frequent in TNBC (89%, 82 of 92) and the HR−/HER2+ subtype (81%, 34 of 42) than in the HR+/HER2− subtype (13%, 6 of 46) ($P < 0.001$).

The incidence of high TIL score (score 3–5) was also higher in TNBC (73%, 67 of 92) and the HR−/HER2+ subtype (55%, 23 of 42) than in the HR+/HER2− subtype (17%, 8 of 46) ($P = 0.002$). An apoptosis score of 2 was also more frequent in TNBC (21%, 19 of 92) and the HR−/HER2+ subtype (48%, 20 of 42) than in the HR+/HER2− subtype (2%, 1 of 46) ($P < 0.001$). The incidences of a basal-like subtype, p53 expression, a high TIL score, and an apoptosis score of 2 did not differ between TNBC and the HR−/HER2+ subtype.

All six metaplastic carcinomas were TNBC [17].

Table 1 Evaluation of clinicopathological parameters in three subtypes of primary breast cancer

	TNBC ($n = 92$) No. of patients (%)	HR−/HER2+ ($n = 42$) No. of patients (%)	HR+/HER2− ($n = 46$) No. of patients (%)	P value
Age				
Median (range)	52 (23-76)	55 (31-71)	55 (31-71)	0.36
T				
1	2 (2)	0 (0)	0 (0)	0.37
2	48 (53)	17 (41)	26 (56)	
3	27 (29)	16 (38)	11 (24)	
4	15 (16)	9 (21)	9 (20)	
N				
0	45 (49)	24 (57)	24 (52)	0.96
1	35 (38)	14 (33)	18 (39)	
2	10 (11)	3 (7)	3 (7)	
3	2 (2)	1 (3)	1 (2)	
Stage				
II	56 (61)	25 (60)	28 (61)	0.99
III	36 (39)	17 (40)	18 (39)	
ER				
Positive	0 (0)	0 (0)	46 (100)	
Negative	92 (100)	42 (100)	0 (0)	
PgR				
Positive	0 (0)	0 (0)	32 (70)	
Negative	92 (100)	42 (100)	14 (30)	
HER2				
Positive	0 (0)	42 (100)	46 (0)	
Negative	92 (100)	0 (0)	0 (100)	
Basal marker				
Positive	54 (59)	18 (43)	3 (7)	<0.001
Negative	38 (41)	24 (57)	43 (93)	
p53				
Positive	58 (63)	26 (62)	12 (26)	<0.001
Negative	34 (37)	16 (38)	34 (74)	
Grade				
1	1 (1)	0 (0)	4 (9)	<0.001
2	9 (10)	8 (19)	36 (78)	
3	82 (89)	34 (81)	6 (13)	
TIL				
Low (0/1/2)	25 (4/8/13) (27)	19 (7/6/6) (45)	38 (25/8/5) (83)	0.002
High (3/4/5)	67 (22/24/21) (73)	23 (8/11/4) (55)	8 (6/2/0) (17)	
Apoptosis				
0	22 (24)	8 (19)	29 (63)	<0.001
1	51 (55)	14 (33)	16 (35)	
2	19 (21)	20 (48)	1 (2)	
pCR (NSABP B-18)				
Yes	29 (32)	9 (21)	3 (7)	0.004
No	63 (68)	33 (79)	43 (93)	
QpCR (JBCRG 01)				
Yes	35 (38)	17 (40)	3 (7)	<0.001
No	57 (62)	25 (60)	43 (93)	
pCR (primary and lymph nodes)				
Yes	26 (28)	6 (14)	3 (7)	0.006
No	66 (72)	36 (86)	43 (93)	

ER estrogen receptor, *HR* hormone receptors, *pCR* pathological complete response, *PgR* progesterone receptor, *TIL* tumor infiltrating lymphocytes, *TNBC* triple negative breast cancer

Table 2 Correlation between therapeutic effect of primary breast cancer to neoadjuvant chemotherapy (NAC) and infiltrating lymphocytes (TIL)

Subtype of breast cancer and response to NAC	No. of patients (%)			*P*
	Total	TIL score		
		0–2	3–5	
A. TNBC				
pCR (NSABP B-18)				
Yes	29 (32)	4 (16)	25 (37)	0.05
No	63 (68)	21 (84)	42 (63)	
QpCR (JBCRG)				
Yes	35 (38)	4 (16)	31 (46)	0.008
No	57 (62)	21 (84)	36 (54)	
pCR (primary + lymph nodes)				
Yes	26 (28)	4 (16)	22 (33)	0.11
No	66 (72)	21 (84)	45 (67)	
B. HR−/HER2+ subtype				
pCR (NSABP B-18)				
Yes	9 (21)	2 (11)	7 (30)	0.12
No	33 (79)	17 (89)	16 (70)	
QpCR (JBCRG)				
Yes	17 (40)	5 (26)	12 (52)	0.09
No	25 (60)	14 (74)	11 (48)	
pCR (primary + lymph nodes)				
Yes	6 (14)	1 (5)	5 (22)	0.13
No	36 (86)	18 (95)	18 (78)	
C. HR+/HER2− subtype				
pCR (NSABP B-18)				
Yes	3 (7)	2 (5)	1 (13)	0.44
No	43 (93)	36 (95)	7 (87)	
QpCR (JBCRG)				
Yes	3 (7)	2 (5)	1 (13)	0.44
No	43 (93)	36 (95)	7 (87)	
pCR (primary + lymph nodes)				
Yes	3 (7)	2 (5)	1 (13)	0.44
No	43 (93)	36 (95)	7 (87)	
D. Total (TNBC+ HR−/HER2+ HR+/HER2−)				
pCR (NSABP B-18)				
Yes	41 (23)	8 (10)	33 (34)	0.0001
No	139 (77)	74 (90)	65 (66)	
QpCR (JBCRG)				
Yes	55 (31)	11 (13)	44 (45)	< 0.0001
No	125 (69)	71 (87)	54 (55)	
pCR (primary + lymph nodes)				
Yes	35 (19)	7 (9)	28 (29)	0.0007
No	145 (81)	75 (91)	70 (71)	

HR hormone receptors, *TNBC* triple-negative breast cancer, *TIL* tumor-infiltrating lymphocyte, *pCR* pathologically complete response, *QpCR* quasi-pCR, *NAC* neoadjuvant chemotherapy

Clinicopathological characteristics and pCR

The pCR rate according to NSABP B-18 classification was significantly higher in TNBC (32%) and HR−/HER2+ subtype (21%) than in HR+/HER2− subtype (7%) ($P = 0.004$). Likewise, the QpCR rate according to JBCRG 01 classification was significantly higher in TNBC (38%) and HR−/HER2+ subtype (40%) than in HR+/HER2− subtype (7%) ($P < 0.001$). Furthermore, the rate of pCR in both primary site and lymph nodes was significantly higher in TNBC (28%) than in HR−/HER2+ (14%) and HR+/HER2− (7%) subtypes ($P = 0.006$) (Table 1).

Table 3 Correlation between apoptosis of tumor cells and therapeutic effect of primary breast cancer to neoadjuvant chemotherapy (NAC)

Subtype of breast cancer and response to NAC	No. of patients (%)			*P*
	Total	Apoptosis		
		Score 0, 1	Score 2	
A. TNBC				
pCR (NSABP B-18)				
Yes	29 (32)	20 (27)	9 (47)	0.10
No	63 (68)	53 (73)	10 (53)	
QpCR (JBCRG)				
Yes	35 (38)	26 (36)	9 (47)	0.35
No	57 (62)	47 (64)	10 (53)	
pCR (primary + lymph nodes)				
Yes	26 (28)	17 (23)	9 (47)	0.04
No	66 (72)	56 (77)	10 (53)	
B. HR−/HER2+ subtype				
pCR (NSABP B-18)				
Yes	9 (21)	4 (18)	5 (25)	0.71
No	33 (79)	18 (82)	15 (75)	
QpCR (JBCRG)				
Yes	17 (40)	7 (32)	10 (50)	0.23
No	25 (60)	15 (68)	10 (50)	
pCR (primary + lymph nodes)				
Yes	6 (14)	2 (9)	4 (20)	0.40
No	36 (86)	20 (91)	16 (80)	
C. HR+/HER2− subtype				
pCR (NSABP B-18)				
Yes	3 (7)	3 (7)	0 (0)	1.00
No	43 (93)	42 (93)	1 (100)	
QpCR (JBCRG)				
Yes	3 (7)	3 (7)	0 (0)	1.00
No	43 (93)	42 (93)	1 (100)	
pCR (primary + lymph nodes)				
Yes	3 (7)	3 (7)	0 (0)	1.00
No	43 (93)	42 (93)	1 (100)	
D. Total (TNBC+ HR−/HER2+ HR+/HER2−)				
pCR (NSABP B-18)				
Yes	41 (23)	27 (19)	14 (35)	0.04
No	139 (77)	113 (81)	26 (65)	
QpCR (JBCRG)				
Yes	55 (31)	36 (26)	19 (47)	0.008
No	125 (69)	104 (74)	21 (53)	
pCR (primary + lymph nodes)				
Yes	35 (19)	22 (16)	13 (32)	0.02
No	145 (81)	118 (84)	27 (68)	

HR hormone receptors, *TNBC* triple-negative breast cancer, *pCR* pathologically complete response, *QpCR* quasi-pCR, *NAC* neoadjuvant chemotherapy

The association between pCR and TIL scores stratified by tumor subtype is shown in Table 2. In patients with TNBC, the pCR rate was significantly higher in those with tumors showing high TIL scores (3–5) (37%, 25 of 67) than in those with tumor showing low TIL scores (0–2) (16%, 4 of 25) ($P = 0.05$). Likewise, the QpCR rate was significantly higher in those with tumors showing the high TIL scores (46%, 31 of 67) than in those with the low TIL scores (16%, 4 of 25, $P = 0.008$). Furthermore, the rate of pCR in both primary tumor and axillary lymph nodes tended to be higher in the patients with tumors showing the high TIL scores (35%, 22 of 67) than in those with tumors

showing the low TIL scores (16%, 4 of 25). A similar tendency of correlation was seen for tumors of HR−/HER2+ subtype (Table 2), although there was no statistic significance. There was no correlation between TIL and therapeutic effect in HR+/HER2− subtype tumors. In a total of 180 cases including all TNBC, HR−/HER2+, and HR+/HER2− subtypes studied, TIL was significantly correlated with pCR, QpCR, and the pCR in both the primary site and lymph nodes ($P = 0.0001$, $P < 0.0001$, and $P = 0.0007$, respectively, Table 2).

In the patients with TNBC, the pCR rate tended to be higher in those with tumors showing an apoptosis score of 2 (47%, 9 of 19) than in those with an apoptosis score 0 or 1 (27%, 20 of 73, $P = 0.10$) (Table 3). Furthermore, the rate of pCR in both primary tumor and axillary nodes was significantly higher in the tumors showing an apoptosis score 2 (47%, 9 of 19) than in those with an apoptosis score 0 or 1 (23%, 17 of 73, $P = 0.04$). A similar tendency of correlation was seen for tumors of HR−/HER2+ subtype (Table 3), although there was no statistic significance between an apoptosis score and these pCRs (Table 3). There was no statistically significant correlation between apoptosis score and therapeutic effect in HR+/HER2− subtype tumors. In a total of 180 cases including these three subtypes, apoptosis was significantly correlated with pCR, QpCR, and the pCR in both the primary site and axillary lymph nodes ($P = 0.04$, 0.008, and 0.02, respectively) (Table 3).

The pCR rate did not differ significantly between p53-negative tumors (13 of 34, 38%) and p53-positive tumors (15 of 57, 26%) in patients with TNBC. In the HR−/HER2+ subtype, however, seven of nine patients who achieved pCR had p53-positive tumors. There was no correlation between pCR and p53 in the HR+/HER2− subtype.

The pCR rate did not differ between patients with tumors of the basal-like subtype and those with tumors of the non-basal-like subtype (Table 4). Same tendencies of relationship with p53 status or with basal-like subtype were seen for the classification of QpCR and for the pCR of both the primary site and axillary lymph nodes (data not shown).

When all 180 cases were combined, T, N, and grade were correlated or tended to be correlated with pCR (Table 4). QpCR, and the pCR of both primary site and axillary lymph nodes also showed similar tendency (data not shown). Age was not correlated with therapeutic effect.

A univariate regression model analysis showed that the high TIL score was significantly correlated with QpCR (relative ratio (RR) 4.52, 95% reliable range (95%RR) 1.40–14.59) and nearly significantly correlated with pCR in

Table 4 Correlation of clinicopathological parameters with pathological complete response (pCR) of primary breast cancer to neoadjuvant chemotherapy

	All	No. of pCR/No. of patients (%)					
		P value	TNBC	*P* value	HR−/HER2+	*P* value	HR+/HER2−	*P* value
Age								
≤50	14/64 (22)	0.80	11/40 (28)	0.46	3/12 (25)	0.72	0/12 (0)	0.39
>50	27/116 (23)		18/52 (35)		6/30 (20)		3/34 (9)	
T								
1, 2	26/93 (28)	0.09	18/50 (36)	0.31	6/17 (35)	0.07	2/26 (8)	0.60
3, 4	15/87 (17)		11/42 (26)		3/25 (12)		1/20 (5)	
N								
Positive	14/87 (16)	0.03	11/47 (23)	0.09	2/18 (11)	0.15	1/22 (5)	0.53
Negative	27/93 (29)		18/45 (40)		7/24 (29)		2/24 (8)	
Stage								
II	31/109 (28)	0.03	21/56 (38)	0.12	8/25 (32)	0.05	2/28 (7)	0.66
III	10/71 (14)		8/36 (22)		1/17 (6)		1/18 (6)	
Grade								
1, 2	7/58 (12)	0.02	3/10 (30)	0.91	1/8 (13)	0.44	3/40 (8)	0.65
3	34/122 (29)		26/82 (32)		8/34 (24)		0/6 (0)	
Basal-like								
Positive	23/75 (31)	0.03	19/54 (35)	0.36	4/18 (22)	0.60	0/3 (0)	0.81
Negative	18/105 (17)		10/38 (26)		5/24 (21)		3/43 (7)	
p53								
Positive	23/95 (24)	0.52	15/57 (26)	0.23	7/26 (27)	0.24	1/12 (8)	0.61
Negative	17/84 (20)		13/34 (38)		2/16 (13)		2/34 (6)	

HR hormone receptors, *pCR* pathological complete response

Table 5 Logistic analysis for prediction of pathological therapeutic effect to neoadjuvant chemotherapy to TNBC

	Relative ratio (95% reliable range)	*P* value
A. Univariate		
1. pCR (NSABP B-18)		
TIL (score 3-5 vs. 0-2)	3.12 (0.96–10.15)	0.058
Apoptosis (2 vs. 0, 1)	2.38 (0.85–6.73)	0.10
2. QpCR (JBCRG)		
TIL (score 3-5 vs. 0-2)	4.52 (1.40–14.59)	0.012
Apoptosis (2 vs. 0, 1)	1.63 (0.59–4.51)	0.35
3. pCR (primary + lymph node)		
TIL (score 3-5 vs. 0-2)	2.57 (0.79–8.39)	0.12
Apoptosis (2 vs. 0, 1)	2.97 (1.04–8.49)	0.043
B. Multivariate		
1. pCR (NSABP B-18)		
TIL (score 3-5 vs. 0-2)	2.78 (0.84–9.18)	0.09
Apoptosis (2 vs. 0, 1)	2.01 (0.70–5.81)	0.20
2. QpCR (JBCRG)		
TIL (score 3-5 vs. 0-2)	4.34 (1.33–14.21)	0.015
Apoptosis (2 vs. 0, 1)	1.27 (0.44–3.65)	0.66
3. pCR (primary + lymph node)		
TIL (score 3-5 vs. 0-2)	2.17 (0.65–7.28)	0.21
Apoptosis (2 vs. 0, 1)	2.60 (0.89–7.58)	0.08

pCR pathological complete response, *TIL* tumor-infiltrating lymphocyte, *TNBC* triple-negative breast cancer

N, *T*, grade, basal-like, p53, and histological type were not significant as predictor of pCR

92 TNBCs (relative ratio 3.12, 95%RR 0.96–10.15) ($P = 0.012$ and 0.058, respectively) (Table 5). Apoptosis was significantly correlated with pCR (primary + lymph node) in 92 TNBCs (RR 2.97, 95%RR 1.04–8.49) ($P = 0.043$). Other parameters, including T, N, grade, basal-like subtype, p53 and histological type, were not significant predictors of pCR. TIL and apoptosis showed no mutual correlation. When these two parameters were subjected to multivariate analysis, only TIL was shown to be a significant independent factor for QpCR (RR 4.34, 95%RR 1.33–14.21, $P = 0.015$), but apoptosis was not significant (Table 5).

Survival analyses

In 92 patients with TNBC, disease-free survival (DFS) curves differed significantly between pCR and non-pCR groups (5-year DFS rate 93% vs. 66%, $P = 0.019$), between QpCR and non-QpCR groups (5-year DFS rate 91% vs. 64%, $P = 0.010$), and between the group of pCR in both primary tumor and axillary lymph nodes and others (5-year DFS rate 92% vs. 68%, $P = 0.043$) (Fig. 3). In TNBC, patients with a high TIL score tumor showed slightly higher 5-year DFS rate than patients with a low TIL score tumor (77% vs. 70%), but the difference was not significant statistically ($P = 0.58$) (Fig. 4).

Discussion

Breast cancer has been shown to be a heterogeneous disease, and each intrinsic subtype of breast cancer differs in terms of gene expression and molecular features [1–5]. Previous studies reported differences between breast cancer subtypes in the pCR rate after primary chemotherapy [8, 10]: Rouzier et al. reported that the pCR rate after anthracycline and taxane chemotherapy in patients with luminal subtypes was 6%, while patients with both the basal-like and erbB2+ (HER2) subtypes had a pCR rate of 45%, based on classification using a "breast intrinsic" gene set [8]. Carey et al. also reported differences in the chemosensitivity of breast cancer subtypes when classified by immunohistochemistry: pCR rates after treatment with anthracycline either alone or in combination with taxane were 27, 36, and 7% for TNBC, and the HER2 and luminal subtypes, respectively [10]. In the present study, we confirmed that the pCR rate, QpCR rate, and the pCR rate in both the primary site and lymph nodes were significantly higher in patients with TNBC and tumors of the HR−/HER2+ subtype than in those with tumors of the HR+/HER2− subtype.

The proportions of cases showing a high TIL score (3, 4 or 5) and high apoptosis (score 2) were larger in TNBC and the HR−/HER2+ subtype than in the HR+/HER2− subtype. In addition, both TIL score and apoptosis were significantly associated with a response to NAC in TNBC, while in the HR−/HER2+ subtype and the HR+/HER2− subtype, these parameters were not significantly associated with pCR or QpCR. Because we used statistical tests on multiple related hypotheses, i.e., pCR, QpCR, and pCR in both the primary tumor and axillary lymph nodes, the data acquired should be considered exploratory. Nonetheless, these results suggest that patients with a high immune response to TNBC were more likely to show pCR, and that the immune component played a substantial role in the response of TNBC to NAC.

Although conflicting results have been reported [20, 21], earlier studies revealed a relationship between high lymphocyte infiltration and good prognosis in patients with breast cancer [22–25]. However, breast cancer subtypes were not taken into consideration in these studies. Kreike et al. demonstrated that a large amount of lymphocytic infiltrate was a significant indicator of longer distant metastasis-free survival in patients with TNBC [26]. In several studies, changes in TIL score or in the percentage in a certain subset of T cells were shown to be correlated

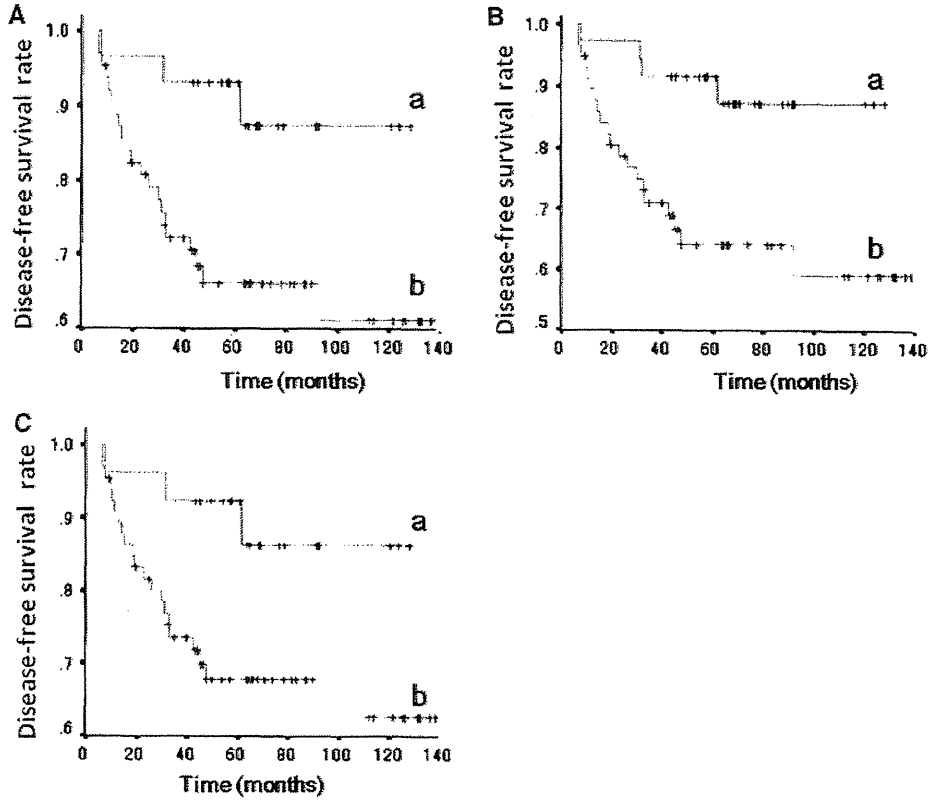

Fig. 3 Disease-free survival curves for patients with primary triple-negative breast cancer (TNBC) after neoadjuvant chemotherapy. **a** Survival curves for (*a*) patient group that showed pCR (NSABP B-18) and (*b*) patient group that showed non-pCR. Curves for two groups are significantly different (5-year DFS rate 93% vs. 66%, $P = 0.019$). **b** Survival curves for (*a*) patient group that showed QpCR (JBCRG) and (*b*) patient group that showed non-QpCR. Curves for two groups are significantly different (5-year DFS rate 91% vs. 64%, $P = 0.010$). **c** Survival curves for (*a*) patient group that showed pCR and (*b*) patient group that showed non-pCR in both primary tumor and axillary lymph nodes and others. *Curves* for two groups are significantly different (5-year DFS rate 92% vs. 68%, $P = 0.043$)

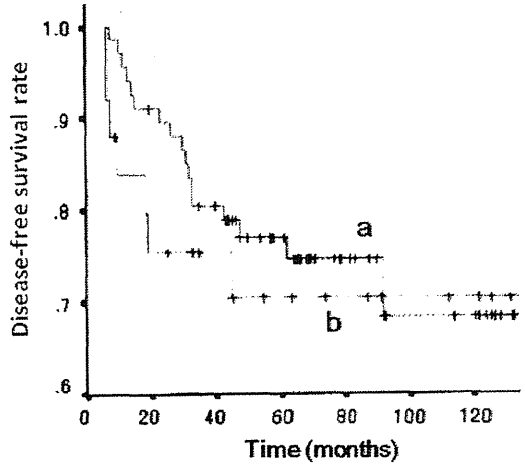

Fig. 4 Disease-free survival curves for patients with primary triple-negative breast cancer (TNBC) after neoadjuvant chemotherapy, stratified by the score of tumor infiltrating lymphocytes (TIL). **a** High TIL score group ($n = 67$). **b** Low TIL score group ($n = 25$). Although the 5-year disease-free survival rate was slightly higher in the high TIL score group (77%) than in the low TIL score group (70%), these two curves did not differ significantly ($P = 0.58$)

with pCR to neoadjuvant chemotherapy of breast cancer [27, 28].

It is also possible that gene expression associated with chemosensitivity and prognosis differs among breast cancer subtypes. Teschendorff et al. also reported that a high level of gene expression representing an immune response was correlated with the better prognosis of patients with ER-negative breast cancer [29]. In fact, Rouzier et al. demonstrated that the genes predictive of pCR differed between the basal-like subtype and the HER2 subtype [8]. Furthermore, Desmedt et al. revealed that the gene expression modules associated with clinical outcome were different between the ER-/HER2− and HER2+ tumors: immune response genes only in the former and both tumor invasion and immune response genes in the latter [5]. Their results were consistent with those of the present study, which demonstrated a significant correlation between the presence of TIL and pCR/QpCR rate in TNBC, but the correlation was only marginal in the HR−/HER2+ subtype. Therefore, the molecular mechanisms determining chemosensitivity may differ between the basal-like and HR−/HER2+ subtypes.

We demonstrated a tendency of correlation between apoptosis and response to NAC in TNBC. Although Desmedt et al. examined the gene expression module associated with apoptosis, there was no association between expression of this gene set and prognosis in any of the breast cancer subtypes examined [5]. Because apoptosis has been defined as programmed cell death, and is usually unaccompanied by inflammation and cytokine release, apoptosis has been believed to be independent of TIL. In

the present study, there was no significant relationship between the presence of TIL and tumor cell apoptosis in TNBC. However, recent studies demonstrated that tumor cell death induced by chemotherapy can promote cytotoxic T-lymphocyte response that confers permanent antitumor immunity [30, 31]. We used histological examination only to identify apoptotic cancer cells. However, it would be more informative to add other techniques, such as the TUNEL method or immunohistochemistry, to identify apoptosis from multiple angles.

We revealed no correlation between the expression of basal-like markers and response to NAC in all of the breast subtypes examined. Although the significance of basal-like markers for clinical outcome is controversial [32–34], a lack of association between basal-like markers and chemosensitivity or prognosis has been demonstrated when breast cancers are divided into subtypes on the basis of ER and HER2 positivity [33, 34]. Nuclear p53 has been shown to be frequent in TNBC [35], but the significance of p53 as a predictive marker for pCR is also controversial [36]. In the present study we were unable to demonstrate any significant impact of p53 as such a marker.

It is unknown whether TILs cause susceptibility to chemotherapy, or they are simply a possible marker of chemosensitivity. There are reports that showed TILs are a predictor of response to neoadjuvant chemotherapy in breast cancer [37, 38]. Hornychova et al. reported that the infiltration of $CD3^+$ T-lymphocytes and $CD83^+$ dendritic cells were correlated with the effectiveness of primary chemotherapy, evaluated as pCR [38]. Denkert et al. showed that T-cell-related markers CD3D and CXCL9 expression were significantly associated with pCR [37]. Several studies suggested possible mechanisms of tumor-immune interaction in response to chemotherapy. pCR to neoadjuvant chemotherapy was shown to be associated with an immunologic profile combining the absence of immunosuppressive $Foxp3^+$ regulatory T cells and the presence of a high number of $CD8^+$ T cells and cytotoxic cells [28]. These reports suggest subsets of TILs caused susceptibility to chemotherapy.

In conclusion, we have demonstrated that the various breast cancer subtypes classified by ER, PgR, and HER2 status have different pathological characteristics and predictive factors for response to chemotherapy. TNBC with a high score for TIL and apoptosis is more likely to respond to chemotherapy. Therefore, in patients with TNBC, the immune response appears to influence on the response to chemotherapy. Further examination is warranted to elucidate the mechanism involved in the immune response component of chemosensitivity.

Acknowledgments We thank Mrs. Sachiko Miura and Mrs. Chizu Kina for excellent technical assistance. This study was supported in part by grants from the Ministry of Health, Labor, and Welfare, Japan, the Ministry of Education, Culture, Sports, Science, and Technology, Japan, and the Princess Takamatsu Cancer Research Fund, Japan.

References

1. Perou CM, Sorlie T, Eisen MB, van de Rijn M, Jeffrey SS, Rees CA, Pollack JR, Ross DT, Johnsen H, Akslen LA, Fluge O, Pergamenschikov A, Williams C, Zhu SX, Lonning PE, Borresen-Dale AL, Brown PO, Botstein D (2000) Molecular portraits of human breast tumours. Nature 406(6797):747–752. doi:10.1038/35021093
2. Sorlie T, Perou CM, Tibshirani R, Aas T, Geisler S, Johnsen H, Hastie T, Eisen MB, van de Rijn M, Jeffrey SS, Thorsen T, Quist H, Matese JC, Brown PO, Botstein D, Eystein Lonning P, Borresen-Dale AL (2001) Gene expression patterns of breast carcinomas distinguish tumor subclasses with clinical implications. Proc Natl Acad Sci USA 98(19):10869–10874. doi:10.1073/pnas.191367098
3. Sorlie T, Tibshirani R, Parker J, Hastie T, Marron JS, Nobel A, Deng S, Johnsen H, Pesich R, Geisler S, Demeter J, Perou CM, Lonning PE, Brown PO, Borresen-Dale AL, Botstein D (2003) Repeated observation of breast tumor subtypes in independent gene expression data sets. Proc Natl Acad Sci USA 100(14):8418–8423. doi:10.1073/pnas.0932692100
4. Carey LA, Perou CM, Livasy CA, Dressler LG, Cowan D, Conway K, Karaca G, Troester MA, Tse CK, Edmiston S, Deming SL, Geradts J, Cheang MC, Nielsen TO, Moorman PG, Earp HS, Millikan RC (2006) Race, breast cancer subtypes, and survival in the Carolina Breast Cancer Study. JAMA 295(21):2492–2502. doi:10.1001/jama.295.21.2492
5. Desmedt C, Haibe-Kains B, Wirapati P, Buyse M, Larsimont D, Bontempi G, Delorenzi M, Piccart M, Sotiriou C (2008) Biological processes associated with breast cancer clinical outcome depend on the molecular subtypes. Clin Cancer Res 14(16):5158–5165. doi:10.1158/1078-0432.CCR-07-4756
6. Hugh J, Hanson J, Cheang MC, Nielsen TO, Perou CM, Dumontet C, Reed J, Krajewska M, Treilleux I, Rupin M, Magherini E, Mackey J, Martin M, Vogel C (2009) Breast cancer subtypes and response to docetaxel in node-positive breast cancer: use of an immunohistochemical definition in the BCIRG 001 trial. J Clin Oncol 27(8):1168–1176. doi:10.1200/JCO.2008.18.1024
7. Nielsen TO, Hsu FD, Jensen K, Cheang M, Karaca G, Hu Z, Hernandez-Boussard T, Livasy C, Cowan D, Dressler L, Akslen LA, Ragaz J, Gown AM, Gilks CB, van de Rijn M, Perou CM (2004) Immunohistochemical and clinical characterization of the basal-like subtype of invasive breast carcinoma. Clin Cancer Res 10(16):5367–5374. doi:10.1158/1078-0432.CCR-04-0220
8. Rouzier R, Perou CM, Symmans WF, Ibrahim N, Cristofanilli M, Anderson K, Hess KR, Stec J, Ayers M, Wagner P, Morandi P, Fan C, Rabiul I, Ross JS, Hortobagyi GN, Pusztai L (2005) Breast cancer molecular subtypes respond differently to preoperative chemotherapy. Clin Cancer Res 11(16):5678–5685. doi:10.1158/1078-0432.CCR-04-2421
9. Dent R, Trudeau M, Pritchard KI, Hanna WM, Kahn HK, Sawka CA, Lickley LA, Rawlinson E, Sun P, Narod SA (2007) Triple-negative breast cancer: clinical features and patterns of recurrence. Clin Cancer Res 13(15 Pt 1):4429–4434. doi:10.1158/1078-0432.CCR-06-3045
10. Carey LA, Dees EC, Sawyer L, Gatti L, Moore DT, Collichio F, Ollila DW, Sartor CI, Graham ML, Perou CM (2007) The triple negative paradox: primary tumor chemosensitivity of breast cancer subtypes. Clin Cancer Res 13(8):2329–2334. doi:10.1158/1078-0432.CCR-06-1109

11. Liedtke C, Mazouni C, Hess KR, Andre F, Tordai A, Mejia JA, Symmans WF, Gonzalez-Angulo AM, Hennessy B, Green M, Cristofanilli M, Hortobagyi GN, Pusztai L (2008) Response to neoadjuvant therapy and long-term survival in patients with triple-negative breast cancer. J Clin Oncol 26(8):1275–1281. doi:10.1200/JCO.2007.14.4147
12. Fisher B, Bryant J, Wolmark N, Mamounas E, Brown A, Fisher ER, Wickerham DL, Begovic M, DeCillis A, Robidoux A, Margolese RG, Cruz AB Jr, Hoehn JL, Lees AW, Dimitrov NV, Bear HD (1998) Effect of preoperative chemotherapy on the outcome of women with operable breast cancer. J Clin Oncol 16(8):2672–2685
13. Toi M, Nakamura S, Kuroi K, Iwata H, Ohno S, Masuda N, Kusama M, Yamazaki K, Hisamatsu K, Sato Y, Kashiwaba M, Kaise H, Kurosumi M, Tsuda H, Akiyama F, Ohashi Y, Takatsuka Y (2008) Phase II study of preoperative sequential FEC and docetaxel predicts of pathological response and disease free survival. Breast Cancer Res Treat 110(3):531–539. doi:10.1007/s10549-007-9744-z
14. Mazouni C, Peintinger F, Wan-Kau S, Andre F, Gonzalez-Angulo AM, Symmans WF, Meric-Bernstam F, Valero V, Hortobagyi GN, Pusztai L (2007) Residual ductal carcinoma in situ in patients with complete eradication of invasive breast cancer after neoadjuvant chemotherapy does not adversely affect patient outcome. J Clin Oncol 25(19):2650–2655. doi:10.1200/JCO.2006.08.2271
15. Rouzier R, Extra JM, Klijanienko J, Falcou MC, Asselain B, Vincent-Salomon A, Vielh P, Bourstyn E (2002) Incidence and prognostic significance of complete axillary downstaging after primary chemotherapy in breast cancer patients with T1 to T3 tumors and cytologically proven axillary metastatic lymph nodes. J Clin Oncol 20(5):1304–1310
16. Elston CW, Ellis IO (1991) Pathological prognostic factors in breast cancer. I. The value of histological grade in breast cancer: experience from a large study with long-term follow-up. Histopathology 19(5):403–410
17. Turner NC, Reis-Filho JS (2006) Basal-like breast cancer and the BRCA1 phenotype. Oncogene 25(43):5846–5853. doi:10.1038/sj.onc.1209876
18. Allred DC, Harvey JM, Berardo M, Clark GM (1998) Prognostic and predictive factors in breast cancer by immunohistochemical analysis. Mod Pathol 11(2):155–168
19. Wolff AC, Hammond ME, Schwartz JN, Hagerty KL, Allred DC, Cote RJ, Dowsett M, Fitzgibbons PL, Hanna WM, Langer A, McShane LM, Paik S, Pegram MD, Perez EA, Press MF, Rhodes A, Sturgeon C, Taube SE, Tubbs R, Vance GH, van de Vijver M, Wheeler TM, Hayes DF (2007) American Society of Clinical Oncology/College of American Pathologists guideline recommendations for human epidermal growth factor receptor 2 testing in breast cancer. J Clin Oncol 25(1):118–145. doi:10.1200/JCO.2006.09.2775
20. Carlomagno C, Perrone F, Lauria R, de Laurentiis M, Gallo C, Morabito A, Pettinato G, Panico L, Bellelli T, Apicella A et al (1995) Prognostic significance of necrosis, elastosis, fibrosis and inflammatory cell reaction in operable breast cancer. Oncology 52(4):272–277
21. Lipponen P, Aaltomaa S, Kosma VM, Syrjanen K (1994) Apoptosis in breast cancer as related to histopathological characteristics and prognosis. Eur J Cancer 30A(14):2068–2073
22. Lee AH, Gillett CE, Ryder K, Fentiman IS, Miles DW, Millis RR (2006) Different patterns of inflammation and prognosis in invasive carcinoma of the breast. Histopathology 48(6):692–701. doi:10.1111/j.1365-2559.2006.02410.x
23. Marques LA, Franco EL, Torloni H, Brentani MM, da Silva-Neto JB, Brentani RR (1990) Independent prognostic value of laminin receptor expression in breast cancer survival. Cancer Res 50(5):1479–1483
24. Nixon AJ, Neuberg D, Hayes DF, Gelman R, Connolly JL, Schnitt S, Abner A, Recht A, Vicini F, Harris JR (1994) Relationship of patient age to pathologic features of the tumor and prognosis for patients with stage I or II breast cancer. J Clin Oncol 12(5):888–894
25. Rilke F, Colnaghi MI, Cascinelli N, Andreola S, Baldini MT, Bufalino R, Della Porta G, Menard S, Pierotti MA, Testori A (1991) Prognostic significance of HER-2/neu expression in breast cancer and its relationship to other prognostic factors. Int J Cancer 49(1):44–49
26. Kreike B, van Kouwenhove M, Horlings H, Weigelt B, Peterse H, Bartelink H, van de Vijver MJ (2007) Gene expression profiling and histopathological characterization of triple-negative/basal-like breast carcinomas. Breast Cancer Res 9(5):R65. doi:10.1186/bcr1771
27. Demaria S, Volm MD, Shapiro RL, Yee HT, Oratz R, Formenti SC, Muggia F, Symmans WF (2001) Development of tumor-infiltrating lymphocytes in breast cancer after neoadjuvant paclitaxel chemotherapy. Clin Cancer Res 7(10):3025–3030
28. Ladoire S, Arnould L, Apetoh L, Coudert B, Martin F, Chauffert B, Fumoleau P, Ghiringhelli F (2008) Pathologic complete response to neoadjuvant chemotherapy of breast carcinoma is associated with the disappearance of tumor-infiltrating foxp3+ regulatory T cells. Clin Cancer Res 14(8):2413–2420. doi:10.1158/1078-0432.CCR-07-4491
29. Teschendorff AE, Miremadi A, Pinder SE, Ellis IO, Caldas C (2007) An immune response gene expression module identifies a good prognosis subtype in estrogen receptor negative breast cancer. Genome Biol 8(8):R157. doi:10.1186/gb-2007-8-8-r157
30. Apetoh L, Ghiringhelli F, Tesniere A, Obeid M, Ortiz C, Criollo A, Mignot G, Maiuri MC, Ullrich E, Saulnier P, Yang H, Amigorena S, Ryffel B, Barrat FJ, Saftig P, Levi F, Lidereau R, Nogues C, Mira JP, Chompret A, Joulin V, Clavel-Chapelon F, Bourhis J, Andre F, Delaloge S, Tursz T, Kroemer G, Zitvogel L (2007) Toll-like receptor 4-dependent contribution of the immune system to anticancer chemotherapy and radiotherapy. Nat Med 13(9):1050–1059. doi:10.1038/nm1622
31. Lake RA, Robinson BW (2005) Immunotherapy and chemotherapy—a practical partnership. Nat Rev Cancer 5(5):397–405. doi:10.1038/nrc1613
32. Cheang MC, Voduc D, Bajdik C, Leung S, McKinney S, Chia SK, Perou CM, Nielsen TO (2008) Basal-like breast cancer defined by five biomarkers has superior prognostic value than triple-negative phenotype. Clin Cancer Res 14(5):1368–1376. doi:10.1158/1078-0432.CCR-07-1658
33. Jumppanen M, Gruvberger-Saal S, Kauraniemi P, Tanner M, Bendahl PO, Lundin M, Krogh M, Kataja P, Borg A, Ferno M, Isola J (2007) Basal-like phenotype is not associated with patient survival in estrogen-receptor-negative breast cancers. Breast Cancer Res 9(1):R16. doi:10.1186/bcr1649
34. Tischkowitz M, Brunet JS, Begin LR, Huntsman DG, Cheang MC, Akslen LA, Nielsen TO, Foulkes WD (2007) Use of immunohistochemical markers can refine prognosis in triple negative breast cancer. BMC Cancer 7:134. doi:10.1186/1471-2407-7-134
35. Bidard FC, Matthieu MC, Chollet P, Raoefils I, Abrial C, Domont J, Spielmann M, Delaloge S, Andre F, Penault-Llorca F (2008) p53 status and efficacy of primary anthracyclines/alkylating agent-based regimen according to breast cancer molecular classes. Ann Oncol 19(7):1261–1265. doi:10.1093/annonc/mdn039
36. Harris LN, Broadwater G, Lin NU, Miron A, Schnitt SJ, Cowan D, Lara J, Bleiweiss I, Berry D, Ellis M, Hayes DF, Winer EP, Dressler L (2006) Molecular subtypes of breast cancer in relation to paclitaxel response, outcomes in women with metastatic disease: results from CALGB 9342. Breast Cancer Res 8(6):R66. doi:10.1186/bcr1622
37. Denkert C, Loibl S, Noske A, Roller M, Muller BM, Komor M, Budczies J, Darb-Esfahani S, Kronenwett R, Hanusch C, von

Torne C, Weichert W, Engels K, Solbach C, Schrader I, Dietel M, von Minckwitz G (2010) Tumor-associated lymphocytes as an independent predictor of response to neoadjuvant chemotherapy in breast cancer. J Clin Oncol 28(1):105–113. doi:10.1200/JCO.2009.23.7370

38. Hornychova H, Melichar B, Tomsova M, Mergancova J, Urminska H, Ryska A (2008) Tumor-infiltrating lymphocytes predict response to neoadjuvant chemotherapy in patients with breast carcinoma. Cancer Invest 26(10):1024–1031. doi:10.1080/07357900802098165

Cancer Science
The official journal of the Japanese Cancer Association

Comparative study of the value of dual tracer PET/CT in evaluating breast cancer

Ukihide Tateishi,[1,7] Takashi Terauchi,[2] Sadako Akashi-Tanaka,[3] Takayuki Kinoshita,[4] Daisuke Kano,[2] Hiromitsu Daisaki,[2] Takeshi Murano,[2] Hitoshi Tsuda[5] and Homer A. Macapinlac[6]

[1]Department of Radiology, Yokohama City University Graduate School of Medicine, Kanagawa; [2]Division of Screening Technology and Development, Research Center for Cancer Prevention and Screening, National Cancer Center, Tokyo; [3]Breast Oncology, Showa University School of Medicine, Tokyo; [4]Division of Breast Surgery and [5]Pathology and Clinical Laboratory Division, National Cancer Center Hospital, Tokyo, Japan; [6]Department of Nuclear Medicine, University of Texas, MD Anderson Cancer Center, Houston, Texas, USA

(Received April 9, 2012/Revised May 22, 2012/Accepted May 22, 2012/Accepted manuscript online May 28, 2012/Article first published online July 4, 2012)

The present study was conducted to assess the relationship between tumor uptake and pathologic findings using dual-tracer PET/computed tomography (CT) in patients with breast cancer. Seventy-four patients with breast cancer (mean age 54 years) who underwent ^{11}C-choline and 2-[^{18}F]fluoro-2-deoxy-D-glucose (^{18}F-FDG) PET/CT prior to surgery on the same day were enrolled in the present study. Images were reviewed by a board-certified radiologist and two nuclear medicine specialists who were unaware of any clinical information and a consensus was reached. Uptake patterns and measurements of dual tracers were compared with the pathologic findings of resected specimens as the reference standard. Mean (±SD) tumor size was 5.9 ± 3.2 cm. All primary tumors were identified on ^{18}F-FDG PET/CT and ^{11}C-choline PET/CT. However, ^{18}F-FDG PET/CT demonstrated focal uptake of the primary tumor with (n = 38; 51%) or without (n = 36; 49%) diffuse background breast uptake. Of the pathologic findings, multiple logistic regression analysis revealed an independent association between fibrocystic change and diffuse background breast uptake (odds ratio [OR] 8.57; 95% confidence interval [CI] 2.86–25.66; P < 0.0001). Tumors with higher histologic grade, nuclear grade, structural grade, nuclear atypia, and mitosis had significantly higher maximum standardized uptake values (SUV_{max}) and tumor-to-background ratios (TBR) for both tracers. Multiple logistic regression analysis revealed that only the degree of mitosis was independently associated with a high SUV_{max} (OR 7.45; 95%CI 2.21–25.11; P = 0.001) and a high TBR (OR 5.41; 95%CI 1.13–25.96; P = 0.035) of ^{11}C-choline PET/CT. In conclusion, ^{11}C-choline may improve tumor delineation and reflect tumor aggressiveness on PET/CT in patients with breast cancer. (*Cancer Sci* 2012; 103: 1701–1707)

Positron emission tomography/computed tomography (PET/CT) with the glucose analog 2-[^{18}F]fluoro-2-deoxy-D-glucose (^{18}F-FDG) is recognized as an important tool in initial tumor evaluation, including staging, in the evaluation of treatment response, and in the assessment of recurrent disease for breast cancer.[1,2] It has been reported that PET/CT adds incremental diagnostic confidence to PET in 60% of patients and in >50% of regions with increased ^{18}F-FDG uptake.[3] Tatsumi *et al.*[4] concluded that PET/CT was preferable in evaluating breast cancer lesions in view of the level of diagnostic confidence that it allows. Regardless of the exact type of PET/CT fusion technique, ^{18}F-FDG uptake in non-malignant conditions often leads to high background uptake on breast imaging.[5]

Histological changes are the cause of considerable variations and false-positive findings on breast imaging. Fibrocystic changes (FCC) are the most common of these conditions that can affect the assessment of imaging features on mammography[6,7] and MRI.[8,9] Similarly, there is evidence in the literature that ^{18}F-FDG PET and accelerated glucose metabolism as a result of FCC lead to false-positive findings and difficulty in determining the boundary of specificity.[10]

Choline is an essential component of the cell membrane and choline uptake is upregulated by choline kinase-α, which catalyses the phosphorylation of choline.[11,12] In mammary epithelial cells, levels of phosphocholine metabolites increase due to overexpression of choline kinase-α, which is regulated by the mitogen-activated protein kinase (MAPK) pathway.[11–13] Recent clinical studies in patients with breast carcinoma undergoing molecular-targeted therapy suggest that ^{11}C-choline uptake is 10-fold higher in aggressive breast carcinoma phenotypes and that the uptake of ^{11}C-choline on PET is correlated with tumor grade.[13] Thus, ^{11}C-choline is considered a promising radiotracer for the evaluation of breast cancer in the clinical setting prior to treatment.

Although both data from ^{18}F-FDG and ^{11}C-choline PET/CT allow more precise evaluation of the primary breast cancer, direct comparisons of these two tracers in breast cancer have not been made. In the present study, we sought to confirm and extend previous findings of ^{11}C-choline PET/CT studies by investigating the association between histological findings and the results of ^{18}F-FDG PET/CT investigations in patients with breast cancer.

Materials and Methods

Patients. Seventy-four patients (mean age 54 years; range 25–89 years) with breast carcinoma were enrolled in the present retrospective dual PET/CT study between March 2008 and March 2010. Patients were eligible for inclusion in the study if they met the following criteria: (i) performance status 0 or 1; (ii) no concomitant malignancy; (iii) histologically proven breast carcinoma diagnosed by biopsy at least 1 month before; and (iv) no history of hormone therapy. All patients were required to provide written informed consent. A regimen of 5-fluorouracil, epirubicin, and cyclophosphamide (FEC) plus paclitaxel was used as neoadjuvant chemotherapy in 32 patients (43%). As a rule, hormone therapy was introduced after completion of imaging studies if needed. Our institutional review board (National Cancer Center Hospital, Tokyo, Japan) approved the present study, which complied with the Health Insurance Portability and Accountability Act. The clinical records of all patients were available for review. All patients received surgery after imaging studies.

Phantom study. A phantom study of PET/CT was performed prior to the clinical study at two institutions to clarify the optimum conditions for data acquisition and to ensure quality control.[14] Studies were performed with a whole-body PET/CT

[7]To whom correspondence should be addressed.
E-mail: utateish@yokohama-cu.ac.jp

doi: 10.1111/j.1349-7006.2012.02348.x

scanner (Aquiduo PCA-7000B; Toshiba Medical Systems, Tochigi, Japan). The CT component of the scanner has a 16-row detector. We used an NEMA image quality (IQ) phantom (NU 2-2001) for cross calibration, because this type of phantom is used in many institutions and data regarding the estimation of the optimum time are available. The radioactivity concentration of the background was set at 2.6 ± 0.2 kBq/mL ^{18}F-FDG, similar to that in clinical settings. The radioactivity concentration of the hot portion was fourfold greater than that of the background. Data were collected over a period of 2–5 min in the dynamic acquisition mode and for 30 min in the static acquisition mode. The data acquired, including normalization data, cross-calibration data, blank scan data, and transmission data, were assessed for visual inspection, phantom noise equivalent count ($NEC_{phantom}$), percentage contrast ($Q_{H,10\ mm}$) and percentage background variability ($N_{10\ mm}$). The preferred parameters pertinent to the clinical condition were $NEC_{phantom} > 10.4$ (counts), $N_{10\ mm} < 6.2\%$, and $Q_{H10\ mm}/N_{10\ mm} > 1.9\%$. After a review of the data analyses, the optimum conditions for the PET/CT were determined as follows: data acquisition, 180 s for one bed; field-of-view, 500 mm; iteration, 4; subset, 14; matrix size,128 × 128; filter, Gaussian 8 mm in full width at half maximum; reconstruction, ordered-subsets expectation maximization (OSEM).

Data acquisition. ^{11}C-Choline was synthesized using a commercially available module, as described by Hara *et al.*[15] Prior to the ^{11}C-choline PET/CT study, patients fasted for at least 6 h. Immediately after they had evacuated their bladder, patients were placed in a supine, arm-up position. For the PET/CT, low-dose CT data were first acquired at 120 kVp using an autoexposure control system (beam pitch 0.875 or 1 and 1.5 or 2 mm × 16-row mode). Data acquisition was performed for each patient from the top of the skull to the mid-thigh. Patients maintained normal shallow respiration during the three-dimensional acquisition of CT scans. No iodinated contrast material was administered. Acquisition of emission scans from the head to the mid-thigh was started 5 min after intravenous administration of a mean ^{11}C-choline dose of 475 MBq (range 469–491 MBq). The ^{18}F-FDG PET/CT study was performed 1 h after the ^{11}C-choline PET/CT study in all patients. Patients received an intravenous injection of 311 MBq (range 197–397 MBq) ^{18}F-FDG with an uptake phase at 64 ± 5 min.

Image interpretation. Dedicated software (Vox-base SP1000 workstation; J-MAC Systems, Sapporo, Japan) was used to review all PET, CT, and coregistered PET/CT images in all standard planes. Images were analyzed visually and quantitatively by two independent reviewers, who recorded their findings after reaching a consensus. A region of interest (ROI) was outlined within areas of increased uptake and measured on each slice. When the lesion was extensively heterogeneous, the ROI was set so as to cover all the components of the lesion. The diffuse pattern of breast was assigned to the breast that shows homogeneous accumulation greater than aortic blood except for the primary lesion. For quantitative interpretations, the standardized uptake value (SUV) was determined according to the standard formula, with activity in the ROI recorded as Bq/mL per injected dose (Bq) per weight (kg), but time decay correction for whole-body image acquisition was not performed. The maximum SUV (SUV_{max}) was recorded using the maximum pixel activity within the ROI. The tumor-to-background ratio (TBR) was calculated with reference to uptake in the contralateral breast.

Pathologic analysis. All patients underwent surgery. Each tumor was staged according to the TNM classification of the International Union against Cancer.[16] Resected specimens were fixed in 10% buffered formalin and embedded in paraffin wax. Then, 4-μm sections were obtained in a plane perpendicular to the long axis of the breast. Paraffin-embedded microslices were stained with H&E. Tissue grading, nuclear grading, and structural grading were done using the grading system of Elston and Ellis.[17] Estrogen receptor (ER) and progesterone receptor status was evaluated using the H-scoring system of McCarty *et al.*[18] Human epidermal growth factor-2 (HER-2/neu) was evaluated by immunostaining with 4B5 primary antibody. Evaluation of the primary lesion was based on the following pathologic findings: FCC, differentiation, subtype, location, diameter of the invasive component, diameter of the non-invasive component, ratio of the invasive component in the tumor (%), tissue grading, nuclear grading, structural grading, nuclear atypia, mitosis, necrosis, fat invasion, cutaneous invasion, muscular invasion, ER status, progesterone receptor status, and HER-2/neu status. In the present study, "non-invasive component" referred to ductal carcinoma *in situ* (DCIS).

Statistical analysis. The Chi-squared test or Fisher's exact probability test were used to compare pathologic findings associated with PET/CT findings. In addition, the Wald test and 95% confidence intervals (CI) were used to evaluate the statistical significance of individual variables. To determine relationships of SUV and TBR between the two tracers, we used Spearman rank correlation. Comparisons of mean values between groups were made using Student's *t*-test or analysis of variance (ANOVA) with Bonferroni's adjustment for multiple comparisons. Parsimonious univariate and multivariate logistic regression models were used to measure independent associations with PET/CT findings. Statistical tests used a two-sided significance level of 0.05. Statistical analyses were performed using PASW Statistics 19 (IBM, Tokyo, Japan).

Results

In all, 74 patients completed the study procedures. The demographic data for all patients are given in Table 1. There were 66 patients (89%) with invasive tumors, 60 of which were ductal carcinoma and six lobar carcinoma. Eight patients (11%) had non-invasive ductal carcinoma.

All primary tumors were identified on ^{18}F-FDG PET/CT and ^{11}C-choline PET/CT (Fig. 1). The SUV_{max} of ^{11}C-choline PET/CT was significantly lower than that of ^{18}F-FDG PET/CT ($P = 0.002$; Table 2). Conversely, the TBR of ^{11}C-choline PET/CT was significantly higher than that of ^{18}F-FDG PET/CT ($P < 0.0001$; Table 2). Using ^{18}F-FDG PET/CT, focal uptake of the primary tumor with ($n = 38$ [51%]; Fig. 2) or without ($n = 36$ [49%]) diffuse background breast uptake was demonstrated. Conversely, ^{11}C-choline PET/CT showed only focal uptake of the primary tumor in all patients. There were

Table 1. Patient demographics

Age (years)	54 ± 13 (24–78)
Tumor side	
Right	44 (59)
Left	30 (41)
Tumor size (cm)	5.9 ± 3.2 (1.8–12.0)
Main location	
Medial upper quadrant	8 (11)
Medial lower quadrant	8 (11)
Lateral upper quadrant	46 (62)
Lateral lower quadrant	6 (8)
Central	2 (3)
Invasive tumor	66 (89)
Non-invasive tumor	8 (11)

Data are given as the mean ± SD, with the range in parentheses, or as the number of patients in each group with percentages in parentheses.

doi: 10.1111/j.1349-7006.2012.02348.x

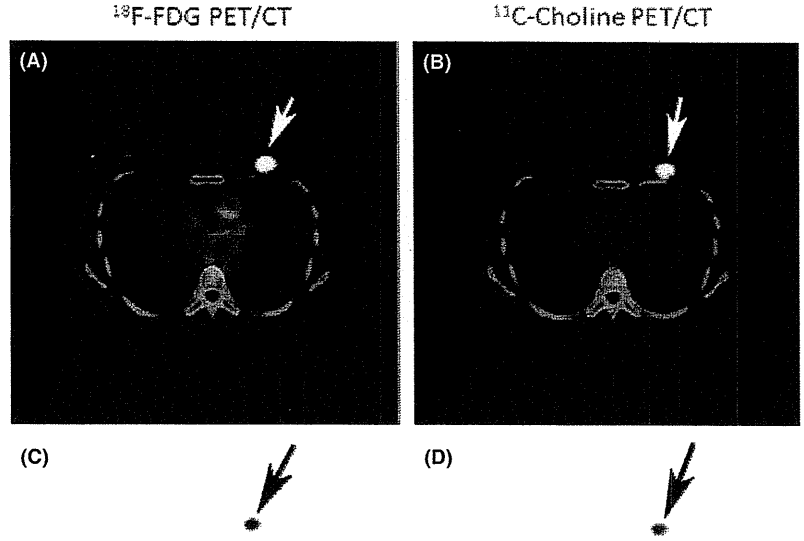

Fig. 1. Results for a 51-year-old woman with invasive ductal carcinoma of the left breast. (a,c) ^{18}F-fludeoxyglucose (FDG) PET/computed tomography (CT) images (fusion image: a; PET alone: (c) reveal a focal hypermetabolic focus in the primary tumor (arrows). The maximum standardized uptake value (SUV_{max}) was 5.5 and the tumor-to-background ratio (TBR) was 47.0. (b,d) Transverse ^{11}C-choline PET/CT images (fusion image: b; PET alone: d) also reveal a focal hypermetabolic focus in the primary tumor (arrows). The SUV_{max} was 5.0 and the TBR was 137.5. On microscopy, the tumor contained 100% invasive component.

Table 2. Computed tomography (CT)/PET measurements and pathologic components with or without diffuse background breast uptake on ^{18}F-fludeoxyglucose PET/CT

	Total	With diffuse uptake	Without diffuse uptake	*P*-value
^{11}C-Choline uptake of tumor				
SUV_{max} (g/mL)	3.7 ± 2.9	3.6 ± 3.5	3.8 ± 2.0	0.789
TBR	8.0 ± 6.0	7.7 ± 9.9	8.3 ± 9.8	0.709
^{18}F-FDG uptake of tumor				
SUV_{max} (g/mL)	4.4 ± 3.1	4.6 ± 3.6	4.2 ± 2.5	0.571
TBR	3.7 ± 2.7	3.2 ± 2.4	4.5 ± 2.9	0.016
Diameter of invasive tumor (cm)	4.1 ± 3.5	4.2 ± 4.0	4.0 ± 3.0	0.800
Diameter of non-invasive tumor (cm)	1.8 ± 2.3	2.6 ± 2.9	0.9 ± 1.0	0.002
% Invasive component	66.0 ± 36.5	54.0 ± 41.4	78.6 ± 25.4	0.003

FDG, fludeoxyglucose; SUV_{max}, maximum standardized uptake value; TBR, tumor-to-background ratio.

significant differences between patients with or without diffuse background breast uptake on ^{18}F-FDG PET/CT for TBR of ^{18}F-FDG (Table 2). There was no interaction between ^{11}C-choline uptake and background breast uptake patterns on ^{18}F-FDG PET/CT. There were significant differences for the diameter of the non-invasive component and the percentage invasive component between patients with and without diffuse background breast uptake on ^{18}F-FDG PET/CT (Table 2).

The pathologic findings and background breast uptake patterns on ^{18}F-FDG PET/CT are listed in Table 3. Patients with diffuse background breast uptake had significantly different values for percentage invasive component, FCC, necrosis, and triple negative tumor compared with patients without diffuse background breast uptake. There were no significant differences between the two groups in histologic grade, nuclear grade, structural grade, nuclear atypia, mitosis, fat invasion, or cutaneous invasion. Nor were there any significant differences in hormone receptor status between the two groups, specifically HER-2/neu, ER, and progesterone receptors. Only FCC showed an independent association with diffuse background breast uptake on multiple logistic regression analysis (OR 8.57; 95% CI 2.86–25.66; $P < 0.0001$).

There was a modest correlation between the diameter of the invasive tumor and SUV_{max} ($P < 0.0001$) or TBR ($P = 0.006$) on ^{18}F-FDG PET/CT (Table 4). Similar trends were found between the diameter of the invasive tumor and SUV_{max} ($P < 0.0001$) and TBR ($P < 0.0001$) on ^{11}C-choline PET/CT (Table 5). The TBR on ^{11}C-choline PET/CT also showed a modest correlation with the percentage invasive component ($P = 0.047$). The diameter of the non-invasive tumor was not correlated with SUV_{max} or TBR on either ^{18}F-FDG or ^{11}C-choline PET/CT.

Pathologic characteristics and tracer uptake are summarized in Table 6. Tumors with a higher histologic grade, nuclear grade, structural grade, nuclear atypia, and mitosis showed significantly higher SUV_{max} and TBR for both ^{18}F-FDG and ^{11}C-choline PET/CT. Tumors without expression of hormone receptors, including ER and progesterone receptors, and triple negative tumors showed significantly higher SUV_{max} and TBR for both ^{18}F-FDG and ^{11}C-choline PET/CT. Tumors expressing FCC and fat invasion were more likely to have high SUV_{max} and TBR on ^{11}C-choline PET/CT, but these differences were not identified in the TBR of ^{18}F-FDG PET/CT. In addition, tumors with necrosis and cutaneous invasion were found to have greater SUV_{max} and TBR only on ^{11}C-choline PET/CT. There was no significant association between the SUV_{max} or TBR and the percentage of invasive component or the HER-2/neu status for both tracers. After adjusting for age and tumor size, multiple logistic regression analysis revealed that the degree of mitosis was independently associated with high

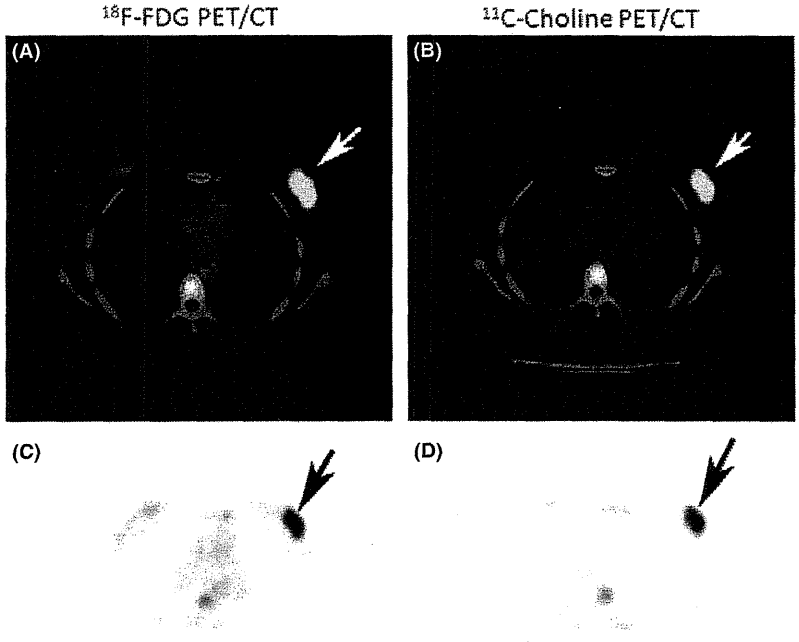

Fig. 2. Results for a 47-year-old woman with invasive scirrhous carcinoma of the left breast. (a,c) ^{18}F-fludeoxyglucose (FDG) PET/computed tomography (CT) images (fusion image: a; PET alone: c) reveal a focal hypermetabolic focus (arrows) of the primary tumor with diffuse background breast uptake. The maximum standardized uptake value (SUV_{max}) was 5.4 and the tumor-to-background ratio (TBR) was 35.7. (b,d) Transverse ^{11}C-choline PET/CT images (fusion image: b; PET alone: (d) reveal only a focal hypermetabolic focus in the primary tumor (arrows). The SUV_{max} was 5.0 and the TBR was 125.0. On microscopy, the tumor contained 15% invasive component. Diffuse fibrocystic changes were found in the background breast.

SUV_{max} (OR 7.45; 95% CI 2.21–25.11; P = 0.001) and high TBR (OR 5.41; 95% CI; 1.13–25.96; P = 0.035) of ^{11}C-choline PET/CT.

Discussion

The present study examined the association between dual-tracer uptake and histological background in breast cancer. Despite positive correlations for SUV_{max} or TBR with ^{18}F-FDG and ^{11}C-choline, mitosis was found to be correlated with ^{11}C-choline uptake only, which reflects tumor aggressiveness reported in the previous study of patients with breast cancer.[19] The results also reveal that diffuse background breast uptake on ^{18}F-FDG PET/CT depends on FCC and this pattern of uptake was not identified in any patients on ^{11}C-choline PET/CT. Our findings suggest that ^{11}C-choline may be feasible for the imaging of breast cancer particularly for patients with underlying FCC in whom mammography and ^{18}F-FDG PET/CT are limited.

Our observation of a positive correlation between mitosis and ^{11}C-choline uptake supports results reported in previous studies.[13,19] This phenomenon was not affected by the underlying histological background because comparative correlation coefficients of SUV_{max} and TBR were similar on ^{11}C-choline PET/CT. Furthermore, the association between mitosis and ^{18}F-FDG uptake was not observed, regardless of positive correlation between ^{18}F-FDG and ^{11}C-choline uptake. This discrepancy in terms of mitosis and tracer uptake in our patients is presumably caused by differences in the degree of tracer uptake.

The present study demonstrated that there were significant differences in the diameter of the non-invasive component and the percentage invasive component between patients with and without diffuse background breast uptake on ^{18}F-FDG PET/CT. However, the SUV_{max} and TBR of both tracers were similar between patients with or without diffuse background breast uptake on ^{18}F-FDG PET/CT. These results suggest that the non-invasive component of breast cancer, which refers to the DCIS component in the present study, cannot be depicted by both tracers. These findings are consistent with that of another study that suggested DCIS could not be precisely visualized by PET.[1] Neubauer *et al.*[20] suggested that the DCIS component could be detected by dynamic contrast-enhanced MRI, but the specificity was unfavorable because of an overlap in kinetic curve appearance. A major limitation of previous studies, as well as the present study, is that whole-body PET/CT scanners were used to evaluate primary lesion of the breast.

Fibrocystic changes are the most common diffuse benign condition of the breast related to changes in responses to estrogen and progesterone. The histology of FCC varies considerably and includes cysts, apocrine metaplasia, fibrosis, calcification, ductal hyperplasia, adenosis, and fibroadenomatous changes.[21,22] Because of its diverse appearances and kinetic features, FCC is major cause of false-positive findings on MRI.[23–25] As for PET studies, Yutani *et al.*[26] have previously explored the ^{18}F-FDG uptake of FCC in 38 patients with breast cancer, providing evidence that diffuse ^{18}F-FDG uptake caused by accompanying FCC obscures uptake by the primary tumor. Palmedo *et al.*[27] have confirmed that FCC is a major cause of reduced specificity in the detection of primary breast cancers on ^{18}F-FDG PET. Furthermore, Kole *et al.*[28] compared the detectability of primary lesions between ^{18}F-FDG PET and ^{11}C-tyrosine PET in patients with breast cancer and concluded that the visual assessment and delineation of the primary tumor were complicated only on ^{18}F-FDG PET when the contralateral breast tissue served as the control because FCC is a bilateral disease. As far as we were aware, the present study is the first that has been designed to evaluate the primary lesion of breast cancer using the dual tracers of ^{18}FDG and ^{11}C-choline. However, considering the high incidence of FCC, PET tracers including ^{11}C-tyrosine and ^{11}C-choline in addition to ^{18}F-FDG are more likely to fulfill specificity expectations.

The exact mechanism of ^{11}C-choline uptake by tumor cells is largely unknown; however, ^{11}C-choline has been proposed as a marker of the extracellular receptor kinase/MAPK pathway, exhibits significant uptake in tumor tissues, and is regarded as a favorable tracer for breast cancer.[13] ^{11}C-Choline uptake may occur via a choline-specific transporter protein that is overexpressed in the cell membranes of breast cancer. ^{11}C-Choline is phosphorylated by choline kinase, which is upregulated in tumor cells for the synthesis of phosphatidylcholine, and is retained within tumor cells.[11,12] Phosphatidylcholine is an essential

doi: 10.1111/j.1349-7006.2012.02348.x

Table 3. Pathologic characteristics and background breast uptake on ^{18}F-fludeoxyglucose PET/computed tomography

	No. patients		*P*-value
	With diffuse uptake	Without diffuse uptake	
Invasive component			
>30%	20	32	0.001
<30%	18	4	
Fibrocystic change			
Present	24	6	<0.0001
Absent	14	30	
Histologic grade			
1 or 2	16	22	0.102
3	22	14	
Nuclear grade			
1 or 2	16	22	0.102
3	22	14	
Structural grade			
1 or 2	14	18	0.253
3	24	18	
Nuclear atypia			
1 or 2	16	20	0.247
3	22	16	
Mitosis			
1 or 2	26	20	0.254
3	12	16	
Necrosis			
Present	22	8	0.002
Absent	16	28	
Fat invasion			
Present	22	24	0.437
Absent	16	12	
Cutaneous invasion			
Present	4	4	0.163
Absent	32	32	
HER-2/neu receptor			
Positive	22	14	0.102
Negative	16	22	
Estrogen receptor			
Positive	28	21	0.163
Negative	10	15	
Progesterone receptor			
Positive	28	21	0.163
Negative	10	15	
Triple negative			
Yes	4	11	0.032
No	34	25	

Table 4. Relationship between ^{18}F-fludeoxyglucose uptake and invasive or non-invasive tumor components

	^{18}F-FDG			
	SUV_{max}	*P*-value	TBR	*P*-value
Diameter of invasive tumor	0.381	<0.0001	0.318	0.006
Diameter of non-invasive tumor	−0.058	0.625	−0.14	0.234
% Invasive component	0.126	0.286	0.189	0.089

FDG, fludeoxyglucose; SUV_{max}, maximum standardized uptake value; TBR, tumor-to-background ratio.

Table 5. Relationship between ^{11}C-choline uptake and invasive or non-invasive tumor components

	^{11}C-Choline			
	SUV_{max}	*P*-value	TBR	*P*-value
Diameter of invasive tumor	0.425	<0.0001	0.537	<0.0001
Diameter of non-invasive tumor	0.038	0.745	−0.066	0.575
% Invasive component	0.125	0.29	0.232	0.047

SUV_{max}, maximum standardized uptake value; TBR, tumor-to-background ratio.

component of cell membranes and is involved in the modulation of transmembrane signaling by carcinogenesis. Therefore, ^{11}C-choline metabolism is accelerated in cell proliferation and is enhanced with increasing tumor grade of breast cancer. In the present study, tumors with higher histologic grade, nuclear grade, structural grade, nuclear atypia, and mitosis showed significantly higher SUV_{max} and TBR for ^{11}C-choline PET/CT. These results are in accord with those of previous *in vivo* and *in vitro* studies.[19,29]

^{11}C-Choline PET/CT has been introduced as feasible method for the evaluation of breast cancer. In the present study, tumors without ER or progesterone receptors and triple negative tumors showed greater uptake of ^{11}C-choline compared with control groups. This suggests that ^{11}C-choline uptake reflects tumor aggressiveness. In a study of 32 patients with pathologically proven breast cancer expressing ER, no association was found between ^{11}C-choline uptake and hormone receptor status.[19] The apparent discrepancy between the present study and those of the previous study[19] may be due, in large part, to differences in the patient populations studied.

In the present study, tumors exhibiting fat invasion were more likely to have a high SUV_{max} and TBR on ^{11}C-choline PET/CT, but these differences were not identified in the TBR of ^{18}F-FDG PET/CT. This appeared to be associated with diffuse ^{18}FDG uptake of breast caused by accompanying FCC, which may obscure tumor delineation. The presence of necrosis or cutaneous invasion was also found to have an association with SUV_{max} and TBR on ^{11}C-choline PET/CT. Overall, our results are consistent with those reported in *in vivo* and *in vitro* studies, in which ^{11}C-choline uptake was found to reflect tumor aggressiveness of breast cancer.[13,19]

The present study design had limitations. First, the present study was designed to assess tumor uptake of dual tracers prior to surgery. The results from a breast cancer patient population of will not fully explain the detectability of advanced or recurrent disease. Second, the present study was an observational study and not a clinical trial, which raises the possibility of confounding factors affecting the results. Third, although ^{11}C-choline is clearly a possible PET tracer for tumor localization in patients with breast cancer, its short half-life restricts its practical application. However, ^{18}F-choline is a tracer with a longer half-life than that of ^{11}C-choline, and so ^{18}F-choline may improve the accuracy of tumor localization. Additional comparative studies regarding detectability and pathologic correlation are needed to validate the findings of the present study. Although we found that ^{11}C-choline uptake reflected tumor aggressiveness in patients with breast cancer, we did not have any data regarding nodal status and follow-up management of the patients. Further studies are needed to clarify the relationship between ^{11}C-choline uptake and patient outcome with a long follow-up period.

In conclusion, the results of the present study suggest that ^{11}C-choline PET/CT allows for the evaluation of tumor aggressiveness and improves delineation of primary tumors compared with ^{18}F-FDG PET/CT in patients with breast cancer. The results demonstrate the advantages and potential of ^{11}C-choline, but clinical evaluation with a long follow-up

Table 6. Pathologic characteristics and tracer uptake

	^{11}C-Choline				^{18}F-FDG			
	SUV_{max}	*P*-value	TBR	*P*-value	SUV_{max}	*P*-value	TBR	*P*-value
% Invasive component		0.979		0.432		0.934		0.79
>30%	3.7 ± 2.3		8.5 ± 5.6		4.4 ± 3.1		3.9 ± 2.4	
<30%	3.7 ± 3.5		7.4 ± 6.4		4.4 ± 3.1		4.1 ± 3.2	
Fibrocystic change		<0.0001		<0.0001		0.002		0.429
Present	5.4 ± 3.5		11.4 ± 6.7		5.7 ± 3.5		4.3 ± 2.2	
Absent	2.5 ± 1.6		5.7 ± 4.0		3.5 ± 2.5		3.8 ± 3.1	
Histologic grade		<0.0001		<0.0001		<0.0001		<0.0001
1 or 2	2.2 ± 1.1		4.4 ± 2.5		2.9 ± 2.0		2.9 ± 2.3	
3	5.3 ± 3.3		11.8 ± 6.2		6.1 ± 3.3		5.2 ± 2.8	
Nuclear grade		<0.0001		<0.0001		<0.0001		<0.0001
1 or 2	2.2 ± 1.1		4.4 ± 2.5		2.9 ± 2.0		2.9 ± 2.3	
3	5.3 ± 3.3		11.8 ± 6.2		6.1 ± 3.3		5.2 ± 2.8	
Structural grade		<0.0001		<0.0001		<0.0001		0.011
1 or 2	2.3 ± 1.5		4.7 ± 3.5		3.0 ± 2.4		3.1 ± 2.7	
3	4.8 ± 3.2		10.5 ± 6.3		5.5 ± 3.2		4.7 ± 2.7	
Nuclear atypia		<0.0001		<0.0001		<0.0001		0.012
1 or 2	2.1 ± 1.1		4.2 ± 2.4		2.8 ± 2.0		2.8 ± 2.3	
3	5.2 ± 3.3		11.6 ± 6.1		5.9 ± 3.2		5.1 ± 2.7	
Mitosis		<0.0001		<0.0001		<0.0001		<0.0001
1 or 2	2.1 ± 1.1		4.5 ± 2.5		2.8 ± 1.8		2.6 ± 2.1	
3	6.4 ± 3.0		13.8 ± 5.5		7.1 ± 3.0		6.3 ± 2.1	
Necrosis		0.046		0.001		0.051		0.529
Present	4.5 ± 3.2		10.6 ± 7.1		5.3 ± 3.3		4.2 ± 2.6	
Absent	3.1 ± 2.6		6.2 ± 4.3		3.8 ± 2.9		3.8 ± 2.9	
Fat invasion		0.003		0.002		0.024		0.061
Present	4.5 ± 3.3		9.6 ± 6.5		5.0 ± 3.4		4.4 ± 2.8	
Absent	2.4 ± 1.5		5.3 ± 3.6		3.4 ± 2.2		3.2 ± 2.6	
Cutaneous invasion		0.004		<0.0001		0.133		0.706
Present	6.4 ± 3.1		14.8 ± 7.3		6.0 ± 4.7		4.3 ± 2.2	
Absent	3.4 ± 2.7		7.2 ± 5.3		4.2 ± 2.8		3.9 ± 2.8	
HER-2/neu receptor		0.53		0.772		0.518		0.766
Positive	3.5 ± 2.6		8.2 ± 6.0		4.2 ± 2.7		4.1 ± 3.1	
Negative	3.9 ± 3.2		7.8 ± 6.0		4.7 ± 3.5		3.9 ± 2.5	
Estrogen receptor		<0.0001		<0.0001		<0.0001		<0.0001
Positive	2.3 ± 1.4		5.4 ± 3.4		3.1 ± 1.8		2.9 ± 2.9	
Negative	6.3 ± 3.3		13.1 ± 6.6		7.0 ± 3.5		6.1 ± 2.5	
Progesterone receptor		<0.0001		<0.0001		<0.0001		<0.0001
Positive	2.4 ± 1.5		5.6 ± 3.7		3.1 ± 1.9		2.9 ± 2.9	
Negative	6.2 ± 3.4		12.7 ± 6.8		7.0 ± 3.5		6.1 ± 2.5	
Triple negative		<0.001		<0.0001		<0.0001		0.002
Yes	6.7 ± 3.3		12.9 ± 6.5		7.4 ± 3.8		6.2 ± 2.1	
No	2.9 ± 2.2		6.7 ± 5.2		3.7 ± 2.4		3.4 ± 2.7	

FDG, fludeoxyglucose; SUV_{max}, maximum standardized uptake value; TBR, tumor-to-background ratio.

period is warranted to clarify the exact role of this technique and how it affects patient outcome.

Acknowledgments

This work was supported, in part, by a Grant-in-Aid for Cancer Research (21–5-2) from the Ministry of Health, Labour and Welfare of Japan.

Disclosure Statement

The authors declare that they have no conflicts of interest.

Abbreviations

CT	computed tomography
DCIS	ductal carcinoma *in situ*
ER	estrogen receptor
FCC	fibrocystic change
^{18}F-FDG2-[^{18}F]	fluoro-2-deoxy-D-glucose
HER-2/neu	human epidermal growth factor-2
MAPK	mitogen-activated protein kinase
SUV_{max}	maximum standardized uptake value
TBR	tumor-to-background ratio

References

1 Nieweg OE, Kim EE, Wong WH *et al.* Positron emission tomography with fluorine-18-deoxyglucose in the detection and staging of breast cancer. *Cancer* 1993; **71**: 3920–5.

2 Rosen EL, Eubank WB, Mankoff DA. FDG PET, PET/CT, and breast cancer imaging. *Radiographics* 2007; **27**: S215–29.

3 Mahner S, Schirrmacher S, Brenner W *et al.* Comparison between positron emission tomography using 2-[fluorine-18]fluoro-2-deoxy-D-glucose, conven-

doi: 10.1111/j.1349-7006.2012.02348.x

tional imaging and computed tomography for staging of breast cancer. *Ann Oncol* 2008; **19**: 1249–54.
4 Tatsumi M, Cohade C, Mourtzikos KA, Fishman EK, Wahl RL. Initial experience with FDG-PET/CT in the evaluation of breast cancer. *Eur J Nucl Med Mol Imaging* 2006; **33**: 254–62.
5 Lim HS, Yoon W, Chung TW *et al.* FDG PET/CT for the detection and evaluation of breast diseases: usefulness and limitations. *Radiographics* 2007; **27**: S197–213.
6 Pisano ED, Johnston RE, Chapman D *et al.* Human breast cancer specimens: diffraction-enhanced imaging with histologic correlation. Improved conspicuity of lesion detail compared with digital radiography. *Radiology* 2000; **214**: 895–901.
7 Venta LA, Wiley EL, Gabriel H, Adler YT. Imaging features of focal breast fibrosis: mammographic–pathologic correlation of noncalcified breast lesions. *AJR Am J Roentgenol* 1999; **173**: 309–16.
8 Chen JH, Liu H, Baek HM, Nalcioglu O, Su MY. Magnetic resonance imaging features of fibrocystic change of the breast. *Magn Reson Imaging* 2008; **26**: 1207–14.
9 van den Bosch MA, Daniel BL, Mariano MN *et al.* Magnetic resonance imaging characteristics of fibrocystic change of the breast. *Invest Radiol* 2005; **40**: 436–41.
10 Yutani K, Shiba E, Kusuoka H *et al.* Comparison of FDG-PET with MIBI-SPECT in the detection of breast cancer and axillary lymph node metastasis. *J Comput Assist Tomogr* 2000; **24**: 274–80.
11 Ishidate K. Choline/ethanolamine kinase from mammalian tissues. *Biochim Biophys Acta* 1997; **1348**: 70–8.
12 Uchida T, Yamashita S. Molecular cloning, characterization, and expression in *Escherichia coli* of a cDNA encoding mammalian choline kinase. *J Biol Chem* 1992; **267**: 10156–62.
13 Kenny LM, Contractor KB, Hinz R *et al.* Reproducibility of [^{11}C]choline-positron emission tomography and effect of trastuzumab. *Clin Cancer Res* 2010; **16**: 4236–45.
14 Fukukita H, Senda M, Terauchi T *et al.* Japanese guideline for the oncology FDG-PET/CT data acquisition protocol: synopsis of Version 1.0. *Ann Nucl Med* 2010; **24**: 325–34.
15 Hara T, Yuasa M. Automated synthesis of [^{11}C]choline, a positron-emitting tracer for tumor imaging. *Appl Radiat Isot* 1999; **50**: 531–3.
16 Sobin LH, Wittekind C. *UICC TNM Classification of Malignant Tumours*, 6th edn. New York: Wiley, 2002.
17 Elston CW, Ellis IO. Pathological prognostic factors in breast cancer. I. The value of histological grade in breast cancer: experience from a large study with long-term follow-up. *Histopathology* 2002; **41**: 154–61.
18 McCarty KS Jr, Szabo E, Flowers JL *et al.* Use of a monoclonal anti-estrogen receptor antibody in the immunohistochemical evaluation of human tumors. *Cancer Res* 1986; **46**: s4244–8.
19 Contractor KB, Kenny LM, Stebbing J *et al.* [^{11}C]choline positron emission tomography in estrogen receptor-positive breast cancer. *Clin Cancer Res* 2009; **15**: 5503–10.
20 Neubauer H, Li M, Kuehne-Held R, Schneider A, Kaiser WA. High grade and non-high grade ductal carcinoma *in situ* on dynamic MR mammography: characteristic findings for signal increase and morphological pattern of enhancement. *Br J Radiol* 2003; **76**: 3–12.
21 Guinebretière JM, Lê Monique G, Gavoille A, Bahi J, Contesso G. Angiogenesis and risk of breast cancer in women with fibrocystic disease. *J Natl Cancer Inst* 1994; **86**: 635–6.
22 Bodian CA, Perzin KH, Lattes R, Hoffmann P. Reproducibility and validity of pathologic classifications of benign breast disease and implications for clinical applications. *Cancer* 1993; **71**: 3908–13.
23 Revelon G, Sherman ME, Gatewood OM, Brem RF. Focal fibrosis of the breast: imaging characteristics and histopathologic correlation. *Radiology* 2000; **216**: 255–9.
24 Orel SG, Schnall MD, LiVolsi VA, Troupin RH. Suspicious breast lesions: MR imaging with radiologic–pathologic correlation. *Radiology* 1994; **190**: 485–93.
25 Fobben ES, Rubin CZ, Kalisher L, Dembner AG, Seltzer MH, Santoro EJ. Breast MR imaging with commercially available techniques: radiologic–pathologic correlation. *Radiology* 1995; **196**: 143–52.
26 Yutani K, Tatsumi M, Uehara T, Nishimura T. Effect of patients being prone during FDG PET for the diagnosis of breast cancer. *AJR Am J Roentgenol* 1999; **173**: 1337–9.
27 Palmedo H, Bender H, Grünwald F *et al.* Comparison of fluorine-18 fluorodeoxyglucose positron emission tomography and technetium-99*m* methoxyisobutylisonitrile scintimammography in the detection of breast tumours. *Eur J Nucl Med* 1997; **24**: 1138–45.
28 Kole AC, Nieweg OE, Pruim J *et al.* Standardized uptake value and quantification of metabolism for breast cancer imaging with FDG and l-[1–11C]tyrosine. *J Nucl Med* 1997; **38**: 692–6.
29 Yoshimoto M, Waki A, Obata A, Furukawa T, Yonekura Y, Fujibayashi Y. Radiolabeled choline as a proliferation marker: comparison with radiolabeled acetate. *Nucl Med Biol* 2004; **31**: 859–65.

Neoadjuvant anastrozole versus tamoxifen in patients receiving goserelin for premenopausal breast cancer (STAGE): a double-blind, randomised phase 3 trial

Norikazu Masuda, Yasuaki Sagara, Takayuki Kinoshita, Hiroji Iwata, Seigo Nakamura, Yasuhiro Yanagita, Reiki Nishimura, Hirotaka Iwase, Shunji Kamigaki, Hiroyuki Takei, Shinzaburo Noguchi

Summary

Background Aromatase inhibitors have shown increased efficacy compared with tamoxifen in postmenopausal early breast cancer. We aimed to assess the efficacy and safety of anastrozole versus tamoxifen in premenopausal women receiving goserelin for early breast cancer in the neoadjuvant setting.

Methods In this phase 3, randomised, double-blind, parallel-group, multicentre study, we enrolled premenopausal women with oestrogen receptor (ER)-positive, HER2-negative, operable breast cancer with WHO performance status of 2 or lower. Patients were randomly assigned (1:1) to receive goserelin 3·6 mg/month plus either anastrozole 1 mg per day and tamoxifen placebo or tamoxifen 20 mg per day and anastrozole placebo for 24 weeks before surgery. Patients were randomised sequentially, stratified by centre, with randomisation codes. All study personnel were masked to study treatment. The primary endpoint was best overall tumour response (complete response or partial response), assessed by callipers, during the 24-week neoadjuvant treatment period for the intention-to-treat population. The primary endpoint was analysed for non-inferiority (with non-inferiority defined as the lower limit of the 95% CI for the difference in overall response rates between groups being 10% or less); in the event of non-inferiority, we assessed the superiority of the anastrozole group versus the tamoxifen group. We included all patients who received study medication at least once in the safety analysis set. We report the primary analysis; treatment will also continue in the adjuvant setting for 5 years. This trial is registered with ClinicalTrials.gov, number NCT00605267.

Findings Between Oct 2, 2007, and May 29, 2009, 204 patients were enrolled. 197 patients were randomly assigned to anastrozole (n=98) or tamoxifen (n=99), and 185 patients completed the 24-week neoadjuvant treatment period and had breast surgery (95 in the anastrazole group, 90 in the tamoxifen group). More patients in the anastrozole group had a complete or partial response than did those in the tamoxifen group during 24 weeks of neoadjuvant treatment (anastrozole 70·4% [69 of 98 patients] *vs* tamoxifen 50·5% [50 of 99 patients]; estimated difference between groups 19·9%, 95% CI 6·5–33·3; p=0·004). Two patients in the anastrozole group had treatment-related grade 3 adverse events (arthralgia and syncope) and so did one patient in the tamoxifen group (depression). One serious adverse event was reported in the anastrozole group (benign neoplasm, not related to treatment), compared with none in the tamoxifen group.

Interpretation Given its favourable risk–benefit profile, the combination of anastrozole plus goserelin could represent an alternative neoadjuvant treatment option for premenopausal women with early-stage breast cancer.

Funding AstraZeneca.

Lancet Oncol 2012; 13: 345–52

Published Online January 20, 2012 DOI:10.1016/S1470-2045(11)70373-4

See Comment page 320

National Hospital Organization, Osaka National Hospital, Osaka, Japan (N Masuda MD); **Sagara Hospital, Kagoshima, Japan** (Y Sagara MD); **National Cancer Center Hospital, Tokyo, Japan** (T Kinoshita MD); **Aichi Cancer Center Hospital, Aichi, Japan** (H Iwata MD); **Showa University Hospital, Tokyo, Japan** (Prof S Nakamura MD); **Gunma Cancer Center, Gunma, Japan** (Y Yanagita MD); **Kumamoto City Hospital, Kumamoto, Japan** (R Nishimura MD); **Kumamoto University Hospital, Kumamoto, Japan** (Prof H Iwase MD); **Sakai Municipal Hospital, Osaka, Japan** (S Kamigaki MD); **Saitama Cancer Center, Saitama, Japan** (H Takei MD); **and Osaka University Graduate School of Medicine, Osaka, Japan** (Prof S Noguchi MD)

Correspondence to: Prof Shinzaburo Noguchi, Department of Breast and Endocrine Surgery, Osaka University Graduate School of Medicine, 2-2-E10 Yamadaoka Suita City, Osaka 565-0871, Japan **noguchi@onsurg.med.osaka-u.ac.jp**

Introduction

For premenopausal women with oestrogen receptor (ER)-positive or progesterone receptor (PgR)-positive breast cancer, treatment options include ablative surgery, radiotherapy, or cytotoxic chemotherapy. Endocrine treatments include the ER antagonist tamoxifen, and luteinising hormone releasing hormone (LHRH) agonists such as goserelin, which offer the potential for reversible ovarian ablation. Goserelin has shown efficacy for the treatment of premenopausal breast cancer, with equivalent disease-free survival to cyclophosphamide, methotrexate, and fluorouracil (CMF) chemotherapy in those patients with ER-positive disease.[1] Although extended goserelin treatment is associated with a known reduction in bone mineral density,[2] it offers a more favourable safety profile than does cytotoxic chemotherapy.[3] The combination of tamoxifen plus goserelin has shown improved progression-free survival compared with goserelin alone;[4] however, a report[5] suggested that the combination of tamoxifen with goserelin was not better than either drug alone (although patients also received concomitant cytotoxic chemotherapy). Present guidelines suggest that tamoxifen alone or with ovarian function suppression are standard treatment options for premenopausal women with ER-positive breast cancer.[6]

Based on the efficacy shown in postmenopausal women with early breast cancer,[7–9] aromatase inhibitors in combination with ovarian suppression are now being assessed for the treatment of premenopausal women with early-stage breast cancer.

Early clinical data in premenopausal women have suggested that the combination of anastrozole and